Impact of Fill-Finish Process on Protein Formulation in the Absence of Stabilizing Agents

BY

Stephanie Kishbaugh

Submitted to the graduate degree program in Pharmaceutical Chemistry and the Graduate Faculty of the University of Kansas in partial fulfillment of the requirements for the degree of Master of Science.

_____

Chair: Dr. Teruna Siahaan,

Aya & Takeru Higuchi Distinguished Professor, Associate Chair

_____

Saeed Moshashaee, Ph.D.

Senior Scientist II, BioMarin Pharmaceutical Inc.

_____

Dr. Michael Hageman,

Valentino J. Stella Distinguished Professor

Date Defended: August 29, 2018

The thesis committee for Stephanie Kishbaugh certifies that this the the approved version of the following thesis:

Impact of Fill-Finish Process on Protein Formulation in the Absence of Stabilizing Agents

_____

Chair: Dr. Teruna Siahaan,

Aya & Takeru Higuchi Distinguished Professor, Associate Chair

Date approved: August 29, 2018

ABSTRACT

Optimization of the fill-finish process for a biotherapeutic is imperative for the highest quality drug product. Chemical and physical degradation must be fully characterized as an enzyme progresses towards commercialization to design a fully optimized process. To avoid degradation and/or sensitivity to the filling process of an enzyme, pharmaceutical scientists utilize stabilizing excipients as tools to mitigate known chemical or structural weaknesses; however, little work has been published on process-related stabilization techniques when the route of administration dictates the exclusion of key stabilizing excipients. The goal of this thesis is to provide guidance in selecting key factors impacting enzyme stability in fill-finish processes in the absence of excipients. The effect of shear stress applied to an enzyme solution was studied in the presence of various interfaces, including air, stainless steel, and tubings commonly used in manufacturing. Although interfacial interactions and aggregation pathways are considered to be enzyme-specific, this work will allow researchers to focus on key conditions affecting stability of proteins in this process. Factors studied here include exposure of the formulation to shear stress from several models with increasing interfacial complexity. The most simplistic model applied a specific shear stress through a microfluidic chip, exposing the enzyme solution to high levels of shear for a short period of time. A cone and plate rotational rheometer was used to study shear applied to an enzyme solution for up to ten minutes with the addition of an air-water interface. Lastly, a recirculation model was employed to study the interaction with tubing surfaces and the shear stresses caused by peristaltic pumping over time. Several analytical assays were employed to understand destabilization caused by these stress models, and were extended to lead to an overall understanding of the impact of various process-related stresses. An enzyme solution exhibits the most dramatic change when exposed to the peristaltic

recirculation pumping model, with the most significantly destabilizing factor being the use of a thermoplastic elastomer tubing surface. The other shear stress models did not produce trends in measured responses, indicating that the associated levels of stress with these models are below the amount necessary to irreversibly alter stability. Methods to measure and characterize aggregation for the recirculation models across a large dynamic range showed dramatic changes with increasing exposure time, resulting in increased aggregate populations over the length of pumping time. The flow imaging data captured high levels of particles shed from the tubing material in the 1-100 µm size-range. These particles could act as heterogeneous nucleation sites, and could explain the increase in aggregation in enzyme solution with these tubing types. The presence of unique multimeric soluble enzyme aggregates was observed in the thermoplastic elastomer tubings, indicating not only that they are deleterious in terms of colloidal stability, but presumably they are formed via different pathways. Silicone tubings performed with a higher standard in recirculation models than thermoplastic tubings. Silicone tubings produced a very low amount of subvisible particulate shedding, undetectable multimeric aggregate species, and a better overall visual appearance after recirculation for up to four hours. In summary, notable enzyme solution instability was not related to the stress of shear in a flow field alone, but rather the use of an incompatible tubing material in the fill-finish process.

ACKNOWLEDGEMENT

First and foremost, I would like to thank my soon-to-be husband Louis Antony Vargas for his everlasting confidence in me and partnership in every way imaginable, without whom I would not have the tools to endure the demands of work, coursework, and research. I also wish to thank my advisor at BioMarin, Dr. Saeed Moshashaee, who has been a source of encouragement and support throughout this process from inception to completion, I am truly fortunate to have been hired by such a supportive and enthusiastic individual, and my career is inspired due to his insight. I thank my KU advisor Dr. Teruna Siahaan for his continued guidance through this process from afar, discussion of data, and endless encouragement. I especially thank Dr. Natalie Ciaccio for introducing me to the Pharmaceutical Chemistry program at KU, and always inspiring me to keep striving for the pursuit of the career I want. I thank my colleagues at BioMarin including Crystal Conlan and Dr. Pooja Sane for the endless support, technical expertise, and confidence boosts throughout the years. I thank my entire formulation development group, led by Dr. Joyce Chou, at BioMarin for their support and encouragement. I thank BioMarin Pharmaceutical for allowing me to advance my education while working, and providing support as a part of their tuition reimbursement program. I acknowledge and thank the members of my thesis committee, Dr. Teruna Siahaan, Dr. Saeed Moshashaee, and Dr. Michael Hageman. I thank the KU Department of Pharmaceutical Chemistry for their support. Lastly, I would like to thank my friends and family for their patience and endless support as I made my way through this program.

TABLE OF CONTENTS

A. INTRODUCTION 1

A.1. Importance of Proteins (Enzymes) as Potential Therapeutics 1

A.2. Importance of Protein Stability during Filling of Primary Packaging: flow and contact-part compatibility 2

B. EXPERIMENTAL SECTION 5

B.1. Reagents and Solutions 5

B.2. Measuring the Effect of Shear using the m-VROC™ 5

B.3. Measuring the Effect of Shear using a Rotational Rheometer 6

B.4. Measuring the Effect of Shear and Process-specific Surfaces during Pumping 7

B.5. Turbidity Measurement 10

B.6. Micro-Flow Imaging 10

B.7. Size-Exclusion Chromatography (SEC) 10

B.8. Reversed Phase Chromatography 11

B.9. Circular Dichroism (CD) Spectroscopy 12

B.10. Dynamic Light Scattering (DLS) 13

C. RESULTS 14

C.1. Calculation of $\gamma'\theta$ Parameter to Normalize Shear Across Platforms 14

C.2. m-VROC™ Results 16

C.3. Rotational Rheometer Results 25

C.4. Recirculated Pumping Model Results 30

D. DISCUSSION 43

E. CONCLUSIONS 52

F. REFERENCES 53

A. INTRODUCTION

A.1. Importance of Proteins (Enzymes) as Potential Therapeutics

Enzymes are integral to many of the mechanisms of human metabolism and health, and it is often devastating when genetic or other forms of disease prevent the body from producing the enzymes needed. Many inherited genetic diseases are caused by the inability of the body to produce certain enzyme(s). Therefore, one of the ways that the field of pharmaceutical sciences has responded is by developing functioning enzyme replacement therapy (ERT) for individuals who have missing or non-functioning enzyme(s). For example, Gaucher disease leads to the buildup of cellular debris in the lysosomes due to the lack of a metabolic enzyme called β-glucocerebrosidase, causing damage to the spleen, liver and bone marrow. In response, several ERT's such as Cerezyme®, VPRIV®, and Elelyso® have been developed and approved to meet this previously unmet medical need. With all the excitement surrounding the promise and development of biotherapeutics, the truth is that enzymes are inherently unstable. Thus, the goal to successfully manufacture, process and provide a suitable shelf-life of an enzyme drug product is not a trivial or inexpensive task for biopharmaceutical companies. This is because enzymes are susceptible to chemical and physical degradation in any of the steps along the manufacturing process up to application in treatment[1].

Chemical and physical degradation pathways are enzyme-specific. An enzyme has a complex structure made up of long chains of uniquely coded amino acids. Each amino acid has its own chemical behavior in solution depending on its identity and location within the primary, secondary, and tertiary structures. A reactive moiety located in an accessible site of the enzyme higher-order structure may undergo a destabilizing chemical reaction, including deamidation, oxidation or a disulfide bond exchange reaction[2]. If any of these modifications were to occur in

a detrimental position, the enzyme could become denatured and no longer maintain its biological activity or therapeutic effect. Physical degradation of a native enzyme involves higher-order conformational changes to form irreversible protein aggregates with different sizes, secondary/tertiary structures, covalent modifications, or morphologies, which can lead to irreversible inactivation of the enzyme[3]. Whatever the resulting classification of aggregates, they produce irreversible agglomeration either with a native monomer, a similarly compromised molecule, or some other impurities[4]. This agglomeration can escalate and eventually grow to the point of becoming insoluble particulate that can even be visible to the eye. To develop the enzyme as a therapeutic agent, it is necessary to fully understand its stability sensitivities during all stages of development, including manufacturing, filling, and packaging processes in order to mitigate them and produce a successfully active drug product[5].

A.2. Importance of Protein Stability during Filling of Primary Packaging: flow and contact-part compatibility

Because fill-finish is the final step in manufacturing a biotherapeutic, it is imperative that the stresses imposed during the process should not lead to aggregation and visible particles in the final drug product. Aggregation can lead to a decrease in potency due to a lower dose in solution and an induction of immunogenicity[6; 7; 8]. The filling process consists of bulk product pooling and aseptic filling via a sterile filtration step through a 0.22 µm pore-size filter. This process requires the transfer of a large amount of liquid drug substance through various tubings and contact parts, imposing stress on the molecule, especially during filtration and filling steps. If aggregates or particulates below the 0.22 µm filter cut-off still remain after filtration, they could act as seeds for nucleation of protein aggregates in the final product during shipping, handling, and storage.

Therefore, it is necessary to fully characterize any undesirable effects of stress generated by pumping or interfacial interactions[9; 10]. In the fluid mechanical sense, shear stress is created by friction between the solution and the tube surface during flow. A shear stress varies linearly across the diameter of tubing with zero shear stress experienced in the center and the maximum shear stress at the wall[11]. Therefore, a constant gradient of movement occurs in a flowing solution containing the enzyme molecules. As the enzyme molecules in solution gain momentum, the incidence of molecular collisions that can compromise protein conformational stability increases. If collisions cause an enzyme to conform to a partially unfolded state, the exposed hydrophobic or chemically labile amino acid residues can promote physical aggregation.

During manufacturing and commercial packaging processes, the drug substance comes into contact with many different types of surfaces. These surfaces can be plastic, glass and steel that are used at various stages of the manufacturing process. It is of utmost importance to ensure that materials used in the final fill-finish process exhibit the highest quality and compatibility profile with low or undetectable leachables or particulates. This is because introduction of leachables can compromise product maximum stability and safety. Bee *et al.*[12] concluded that destabilization of protein in formulation could be mitigated to produce the best outcome by formulation adjustments, process modifications, or material changes. For the formulation presented herein, process and material changes are the only opportunity to produce the best outcome.

The goal of this work was to observe the effects of both shear stress and tubing interfacial interactions on the stability of an enzyme in the absence of sugar or surfactant with the intent to design an optimized fill-finish process. To study increasingly complex applications of shear, models were developed using a pressure differential viscometer, the m-VROC™, a rotational rheometer using cone and plate geometry, and a peristaltic pumped recirculation model with

commonly used tubing materials. Various analytical tools were used to elucidate enzyme instability, including RP-HPLC, SEC-HPLC, CD, DLS, MFI, and turbidity measurements. Although shear stress does not significantly influence the enzyme stability, the clearest factor causing instability was the exposure to a specific tubing surface. The interactions of enzyme solution with various marketed tubing materials produced different outcomes when pumped in the recirculation model presented here. The results showed that there is an advantage of using one material over another; thus, the selection of tubing material should be considered and tested carefully when designing the filling process.

B. EXPERIMENTAL SECTION

B.1. Reagents and Solutions

The enzyme used in this study was formulated at a 30 mg/mL protein concentration in Sodium Phosphate buffer at pH 6.5, including various salts found in the intracerebral space including Sodium Chloride, Potassium Chloride, Calcium Chloride, and Magnesium Chloride, called artificial cerebral spinal fluid, or aCSF buffer. aCSF buffer used in the pumping experiments was identical to the enzyme biotherapeutic formulation buffer solution without the enzyme. The enzyme was provided by BioMarin Pharmaceutical Inc. (Novato, CA, USA).

All salts used were purchased from VWR® (Radnor, PA, USA) with a multicompendial grade. Salts used to prepare SEC-HPLC mobile phase and formulation buffers were purchased from VWR® (Radnor, PA, USA). All solvents and solutions used for RP-HPLC including Tween-20, Methanol (MeOH), Sodium Hydroxide (NaOH), Acetonitrile (ACN), HPLC-grade water, and Trifluoroacetic acid (TFA) were obtained from Sigma-Aldrich® (St. Louis, MO, USA).

B.2. Measuring the Effect of Shear using the m-VROC™

The stress experiment was carried out once using the pressure differential m-VROC™ Viscometer (Rheosense, San Ramon, CA, USA) and was the most highly controlled system for applying a shear stress. The m-VROC™ is a closed system comprised of a glass gastight syringe connected to a stainless steel channel chip, mVROC-C05, equipped with several pressure sensors, which provide feedback to measure various properties of the solution at a controlled temperature. The test was performed in the absence of an air interface, allowing for the accurate

exposure of a solution to very high shear rates for a short burst of time. The only surfaces that the biotherapeutic encountered were a gastight borosilicate type I glass of the 10 mL syringe with a PTFE plunger and a stainless steel channel inside the chip for measuring pressure.

The shear rates experienced by the protein formulation were high, up to 200 ks^{-1}; but because the internal volume of the chip was only 1.2 mm^3, the residence time was short, leading to a $\gamma'\theta$ parameter in the range of 10^3.

B.3. Measuring the Effect of Shear using a Rotational Rheometer

A Bholin CVO100 cone and plate rheometer (Malvern, Malvern, UK) was used to expose the biotherapeutic enzyme to both shear and an air interface, which is known to be a factor for causing protein damage or aggregation[13; 14]. 1.2 mL of the neat 30 mg/mL enzyme was introduced to a 4/40 cone and plate system lowered to a 150 mm gap height. Once the enzyme solution was introduced and allowed to thermally equilibrate for 2 minutes, the system was brought to a constant shear rate for 10 minutes. The sample was collected directly after the application of a constant shear rate for analysis using various assays described in the analysis section (see below).

The enzyme test solution was held in place by surface tension and the solution was exposed to an air interface along the height of the gap between the cone and the plate. As the cone begins to apply a constant shear rate, the rate should stay below the test-solution point of ejection. The enzyme solution was water-like; therefore, the shear rates applied by the rotational rheometer were lower than the mVROC™ with the maximum shear rate at 1 x 10^3 s^{-1}. The limitation of the relatively lower shear rate applied was balanced by the application of a 10-minute exposure

time, which was long in comparison to the mVROC™ and it was only limited by rate of evaporation from the air interface. This method led to a $\gamma'\theta$ parameter ranging from 10^3 to 10^5.

B.4. Measuring the Effect of Shear and Process-specific Surfaces during Pumping

The pumping process of the enzyme solution was the most complex system to assess and model; this was due to the presence of interfacial phenomena experienced by the enzyme solution as well as the stress of flow applied by a peristaltic pump. All experiments were completed in a laminar flow biosafety cabinet to minimize external particulate introduction to the system. A peristaltic Flexicon PF6 pump, (Watson Marlow, Wilmington, MA, USA) was calibrated to dispense 5.4 mL, using a specific gravity of 1.0148 and a 2-second pause time. Biotherapeutic enzyme solution at 30 mg/mL or aCSF buffer was measured and added to a particle-free, sterile 50 mL conical container for recirculation and a new piece of treated tubing was used for each experimental replicate. Solution was continuously pumped through 1-meter of tubing at 100 RPM. As each time point was reached (*i.e.*, 15 min, 60 min, 120 min, 180 min and 240 min), 2 mL of solution was removed for analysis. Samples were immediately frozen at -50 °C and held until analysis was performed.

Tubing was prepared by cutting into 1-meter segments followed by a rinsing with Milli-Q water, and then it was dried with Nitrogen gas to remove any settled particles from the contact surface. After drying, all tubing segments were autoclaved at 121 °C for 30 min and cooled prior to use. To expose the enzyme solution to different shear rates, two different tubing inner-diamaters (IDs) were used in these experiments: 1.6 mm and 3.2 mm. The 1.6 mm ID tubing was used to represent the worst-case or high-stress flow dynamics with a caculated $\gamma'\theta$ parameter

range of 10^6 to 10^7. The 3.2 mm ID tubing had a caculated $\gamma'\theta$ parameter range of 10^5 to 10^6. Tubing types and their characteristics are summarized in Table 1.

It is important to note that the PureWeld®XL tubing was difficult to use in the peristaltic pump as its outer surface was smooth, causing the tubing segment to travel in the pump head over time, even with the use of the appropriately sized holding block. To keep the tubing in place during the recirculation experiment, it had to be bent and taped to the pump itself to prevent from slipping. Additionally, at every time point, it was often repositioned and re-taped to ensure the tubing did not move from the recirculation vessel over time to introduce unwanted air interfaces into the solution.

Table 1. Tubings investigated and their properties				
Manufacturer	Identity	Physical Properties		
		Chemistry Type	Durometer[1]	Comment
Saint-Gobain[2]	Sani-Tech® ULTRA	Platinum-cured Silicone	50	-
	Sani-Tech® STHT		50	-
Watson-Marlow[3]	PureWeld® XL	Thermoplatic Elastomer	65-70	Smooth/slippery Opaque
Saint-Gobain	PharMed® BPT		64	Opaque/cream colored

[1]Durometer is a measure of material hardness
[2]Watson Marlow, Wilmington, MA, USA
[3]Saint-Gobain, Malvern, PA, USA

Table 2. RP HPLC method gradient					
a) Sample Method Gradient			b) Column Cleaning Gradient		
Time (min)	%B	Flow Rate (mL/min)	Time (min)	%B	Flow Rate (mL/min)
0	10	0.75	0	10	0.5
3.5	32	0.75	2.8	10	0.5
15	55	0.75	3	10	1
18.5	55	1.3	6.5	52	1
20.5	10	1.3	10	70	1
26	10	1.3	12.5	70	1.3
			17	10	1.3
			22	10	1.3

B.5. Turbidity Measurement

The overall aggregation was monitored by measuring absorbance at 550 nm using a SpectraMax M2e Microplate reader (Molecular Devices, Sunnyvale, CA, USA). 200 µL of neat protein solution was pipetted to a 96-well transparent plate for measurement.

B.6. Micro-Flow Imaging

Subvisible particulate analysis was carried out using either an MFI5200 or MFI4200 instrument (ProteinSimple, San Jose, CA, USA) in conjunction with MVSS software. Approximately 0.75 mL of either the neat protein or buffer test sample was loaded into the instrument with a 1 mL pipette tip. The sample volume then flowed through a 100 µm (SP3), 1.6 mm Silane coated flow cell (Part No. 4002-002-001) for analysis. The instrument suitability check was performed using a 5 µm Duke Standard™ bead (Thermo Scientific™, Waltham, MA, USA). The flow cell was flushed with 15–25 mL of particle-free water after each measurement run, and a water check was performed to confirm flow cell cleanliness with a criteria of < 200 particles/mL between every run. Protein samples were run neat except those with a highly visible turbidity. Pumped samples with high turbidity were diluted 1:5 using particle free aCSF buffer to ensure accurate particle counting.

B.7. Size-Exclusion Chromatography

Quantitative analyses of monomer and soluble higher order molecular weight aggregates were determined using a Waters HPLC system with column heater, sample refrigeration,

continuous mobile phase degasser, auto injector, and UV detector (Waters, Orlando, FL, USA). Protein solution was diluted to 1 mg/mL in formulation buffer and pre-filtered using a 0.2 µm PVDF filter (MilliporeSigma®, Burlington, MA, USA). Finally, 20 µg in 20 µL of each test sample was injected onto a TSK gel G3000SWxl, 7.8 x 30 cm column (Tosoh Bioscience, South San Francisco, CA, USA). An isocratic method was used at 1 mL/min for 25-minute run time in a 10 mM Sodium Phosphate, 300 mM NaCl Mobile Phase at pH 7.4, monitored at 214 nm. The protein peaks were integrated using Empower3 software (Waters, Orlando, FL, USA) and the result for each experiment was reported as % Area normalized to the unstressed or the initial protein peak.

B.8. Reversed Phase Chromatography

Quantitative analyses of monomer and various chemical degradant contents was performed using a polystyrene-divinylbenzene (PS-DVB) reversed-phase column: 4000Å, 5 µm particle size, and 50 x 4.6 mm column (Agilent Technologies, Santa Clara, CA, USA). At the time of analysis, the assay was unqualified and meant to aid only in viewing a change in the "post-peak." Although identity of the degradation peaks was unestablished at the time; these degradants had previously been implicated in some forced degradation studies (data not shown). Results are reported as % Area, and are normalized to the initial, or unstressed protein for each experimental replicate as some variability has been seen with the results.

A Waters® Alliance HPLC system was used, equipped with a column heater set at 50 ± 2 °C, sample refrigeration set at 6 ± 3 °C, a continuous mobile phase degasser, auto injector, and a UV detector monitoring 214 nm (Waters®, Orlando, FL, USA). Chromatograms were integrated

using Empower3 software, (Waters®, Orlando, FL, USA). Neat protein solution was diluted to 1 mg/mL in aCSF formulation buffer and pre-filtered using a 0.2 µm PVDF syringe filter (MilliporeSigma®, Burlington, MA, USA).

Samples were prepared for injection by mixing 20 µL of the diluted and filtered 1 mg/mL protein, 20 µL 0.05% v/v Tween-20, and 160 µL 500 mM Tris base with 0.05% Tween-20 solutions. 30 µL of this sample mixture was injected onto the column using a gradient method as described in Table 2. Mobile phase A was comprised of 90% Water, 10% ACN with 0.1% TFA, and mobile phase B was comprised of 80% ACN, 20% Water, and 0.09% TFA. Each sample injection was followed by a 100 µL injection of cleaning solution, which was comprised of 1.0 M NaOH with 20% MeOH run using the column cleaning gradient found in Table 2.

B.9. Circular Dichroism (CD) Spectroscopy

CD spectra were collected using a J-1500 CD (Jasco, Tokyo, Japan) equipped with a Peltier element and an autosampler. CD spectra (285–195 nm) were measured in a 0.1 mm quartz cell with a scanning speed of 20 nm/min, a D.I.T. of 4 sec, a data pitch of 0.5 mm, and 1 nm bandwidth. Sample spectra were averaged over 2–3 accumulations and buffer correction was applied by subtraction using the aCSF buffer spectrum. The molar ellipticity was calculated using a molecular weight of 68 kDa in the Spectra Analysis software (Jasco®, Tokyo, Japan). Samples were prepared by diluting the neat enzyme sample with aCSF buffer to either 0.5 or 1 mg/mL concentration, for the 1 mm and 0.1 mm flow cell, respectively. Sample solutions were not filtered prior to data collection.

B.10. Dynamic Light Scattering (DLS)

A Zetasizer-APS (Malvern, Malvern, UK) was used for size measurement analysis of protein samples. Protein samples were diluted to 1 mg/mL using aCSF buffer and filtered using a 0.2 µm syringe filter (MilliporeSigma®, Burlington, MA, USA) prior to loading 75 µL onto a 96-well plate for analysis.

C. RESULTS

C.1. Calculation of γ'θ Parameter to Normalize Shear Across Platforms

Three different models were used to apply a shear stress and the unitless γ'θ parameter was determined for each method using Equation 1 to allow for a comparison across methods. Each type of experiment was performed with increasing complexity, allowing the γ'θ parameter to distinguish interfacial factors from shear stress alone across the models used. This term takes into account the applied shear rate and applied stress time, which both are important parameters to compare among models, and was used by Charm and Lai[15] to highlight that importance.

Equation 1: $\gamma'\theta = shear\ rate, s^{-1}\ (\gamma') \times exposure\ time, s\ (\theta)$

The calculation of γ'θ parameter in m-VROC™ required an understaning of the residence time inside the mVROC-C05 chip to arrive at the θ parameter for Equation 1. The shear stress experienced by the enzyme solution during travel through the inlet and outlet tubing of the chip was assumed to be negligible because the inner diameter of each tubing was large compared to the channel in the chip itself. Therefore, to find θ, the volume of the chip as 0.0012 cm^3 was divided by the volumetric flow rate associated with each shear rate tested, which was provided by the m-VROC™ software. Although the shear rates tested increased from 5 to 200 ks^{-1}, the γ'θ parameter for this method at all shear rates was 1.6 x 10^3. In this model, a decrease in the θ parameter was compensated by an increase in γ', resulting in the same γ'θ parameter for each rate tested. Theoretically, equal amounts of protein degradation should be observed for each rate tested, assuming there is no effect of contact surface interaction with increasing surface exposure

time. With a residence time ranging from ~8 milliseconds to 0.3 seconds, it is unlikely that surface interactions play a role in the degradation observed in this model.

The rotational rheometer application of shear stress included an air-water interface, introducing a new factor which could cause enzyme degradation. The rotational rheometer $\gamma'\theta$ parameter calculation included shear rates (γ') of 5,500 or 1,000 s^{-1}, which is multiplied by 600 seconds as a total time for the stress exposure. Therefore, the $\gamma'\theta$ parameters from this model were 3×10^3, 3×10^5, and 6×10^5.

The recirculate pumping model was the most complex system out of all experiments. To simplify the model, the shear rate used for the $\gamma'\theta$ parameter was calculated utilizing the shear stress experienced at the wall (τ_w) of the tubing, representing the worst-case shear, as the shear stress experienced by the solution should be at the highest level on the wall in laminar flow[16]. Thus τ_w, can be calculated using Equation 2.

$$\text{Equation 2:} \quad \tau_w = \frac{R}{L} \times \frac{\Delta P}{2}$$

where, R is the internal radius of the tubing, L represents the tubing length, and ΔP is the pressure drop across the tubing. ΔP was caculated using Equation 3[16], below.

$$\text{Equation 3:} \quad \Delta P = \frac{8 \times \mu \times L \times V}{\pi R^4}$$

where μ is dynamic viscosity, L is length of tubing, V is volumetric flow rate, and R is internal radius of the tubing. The dynamic viscosity used was measured by the m-VROC™. Finally, the shear stress at the wall, τ_w, can be related to shear rate by Equation 4.

$$\text{Equation 4:} \quad Shear\ Rate\ (\gamma') = \frac{Shear\ stress\ at\ the\ wall\ (\tau_w)}{Viscosity\ (\mu)}$$

With a consistent RPM setting for the peristaltic pump, the shear rate will be identical for tubings of the same ID and length. Therefore, to adjust the shear rate experienced by the system, two different inner diameter (ID) tubings were used (*i.e.*, ID = 3.2 mm and 1.6 mm). Conveniently, these are also common tubing sizes used in fill-finish manufacturing practices. Additionally, the $\gamma'\theta$ parameter was adjusted to cover a very large range by varying the time recirculated. The final calculated $\gamma'\theta$ parameters for the tubing recirculation model of this study for both tubing sizes can be seen in Table 3 (see below). A high-level overview of the results from each of the models in terms of each analytical method's ability to measure changes induced into the system were summarized in Table 4.

C.2. m-VROC™ Results

The effect of a $\gamma'\theta$ parameter of 1.6×10^3 was investigated using DLS by plotting shear rates (γ') *vs.* Z Average (nm) and shear rates *vs.* polydispersity index (Figure 1a). Shear rates tested ranged from 5,000 s^{-1} to 200,000 s^{-1} in a single experiment at 20 °C. There were no changes observed in both Z Average and polydispersity index at various shear rates using m-VROC™ method (Figure 1a), indicating no measurable global destabilization during the specific contact and stress application. The formation of dimer in solution during stress at different shear rates was also monitored by SEC (Figure 1b). The result showed that there was no change in the dimer percent area as the shear rates increased.

The stressed enzyme solution was also analyzed for changes in secondary structure using CD (Figure 2a) across all shear rates tested. Spectra were collected from 285–195 nm, and the presence of two molar ellipticity minima at 208 nm and 220 nm indicate α-helical secondary structure. Qualitatively, no change in conformation appear when exposed to different shear rates

experienced by this model, as indicated by the Figure 2a overlay. Lastly, the effect of shear rate on SVP formation was tested using the MFI (Figure 2b). Total subvisible particle did not show any increase with an increase in shear rate applied to the solution. The overall SVP concentration hovered around the method's LOD (200 particles/mL), indicating very low levels of SVP's. Because these solutions were clear upon visual inspection, it can be concluded that no higher-order insoluble aggregation occurred during the m-VROC™ application of a shear stress to the solution. Results from all methods are consisent, and support the claim that a $\gamma'\theta$ parameter of 1.6×10^3 alone does not cause measurable enzyme destabilization.

Table 3. γ'θ parameters calculated for pumping experiments		
Time (s)	1.6 mm Tubing γ'θ	3.2 mm Tubing γ'θ
900	1.3E+06	5.1E+05
3600	5.1E+06	2.1E+06
7200	1.0E+07	4.1E+06
10800	1.5E+07	6.2E+06
14400	2.0E+07	8.2E+06

Table 4. Methods of analysis and their produced response			
Endpoints/ Methods of Analysis	m-VROC™	Rotational Rheometer	Recirculation Pumping Model
Subvisible Particle Count (MFI)	-	-	+
Turbidity (OD 550)	NT	NT	+
Particle size/Homogeneity (DLS)	-	-	+
Percent Dimer/Multimer (SEC-HPLC)	-	-	+
Percent Post-Peak (RP-HPLC)	NT	-	-
Secondary Structure (CD)	-	-	-

NT: Not Tested

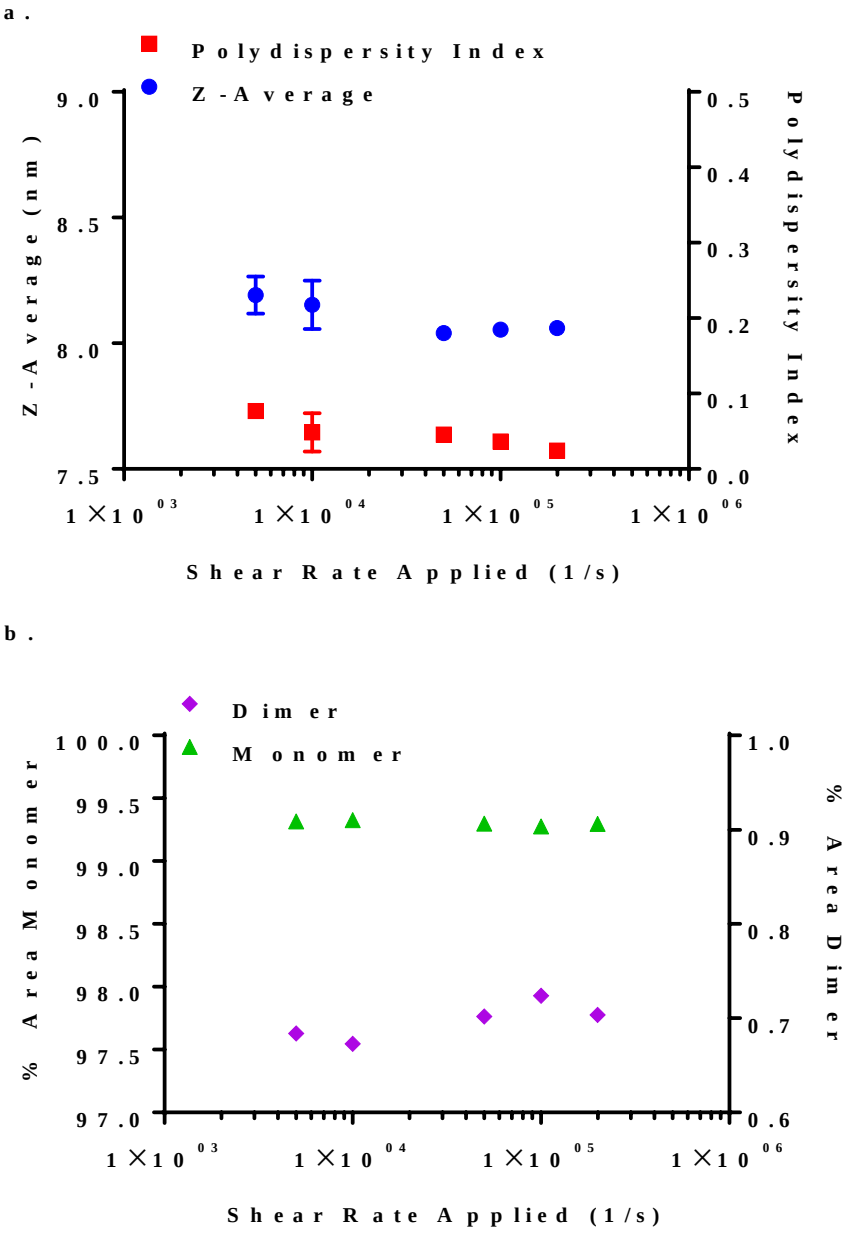

Figure 1. Effect of shear on the physical properties of the enzyme evaluated using m-VROC™ experiment. (a) Overlayed graphical representation between polydispersity index and Z average from dynamic light scattering experiments. (b) Overlayed of between % monomer and dimer detected using SEC HPLC.

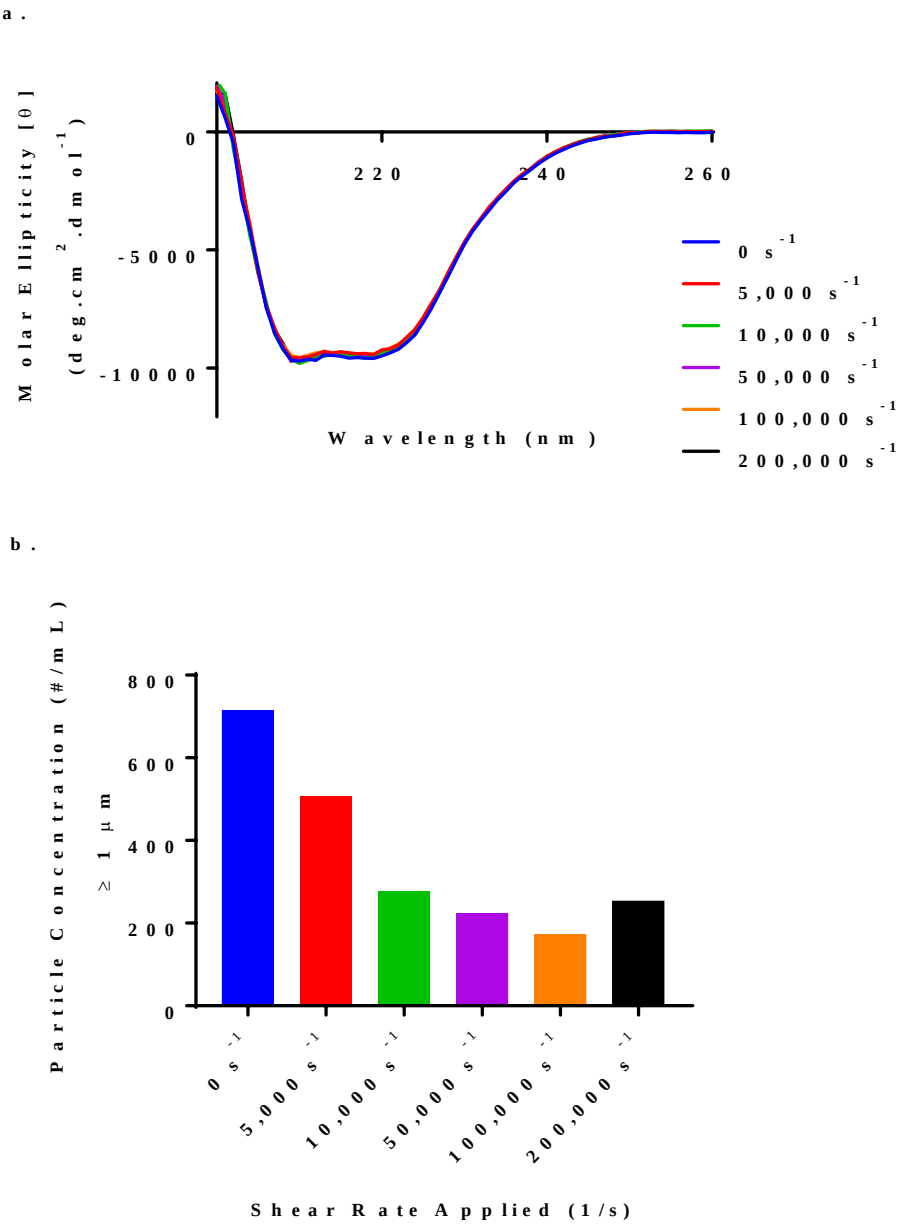

Figure 2. The effect of stress at different shear rates on neat enzyme solution evaluated using m-VROC™. (a) The effect on the secondary structure of the enzyme was measured by CD absorption. (b) The effect on total the concentration of subvisible particles of neat protein solution was determined by MFI.

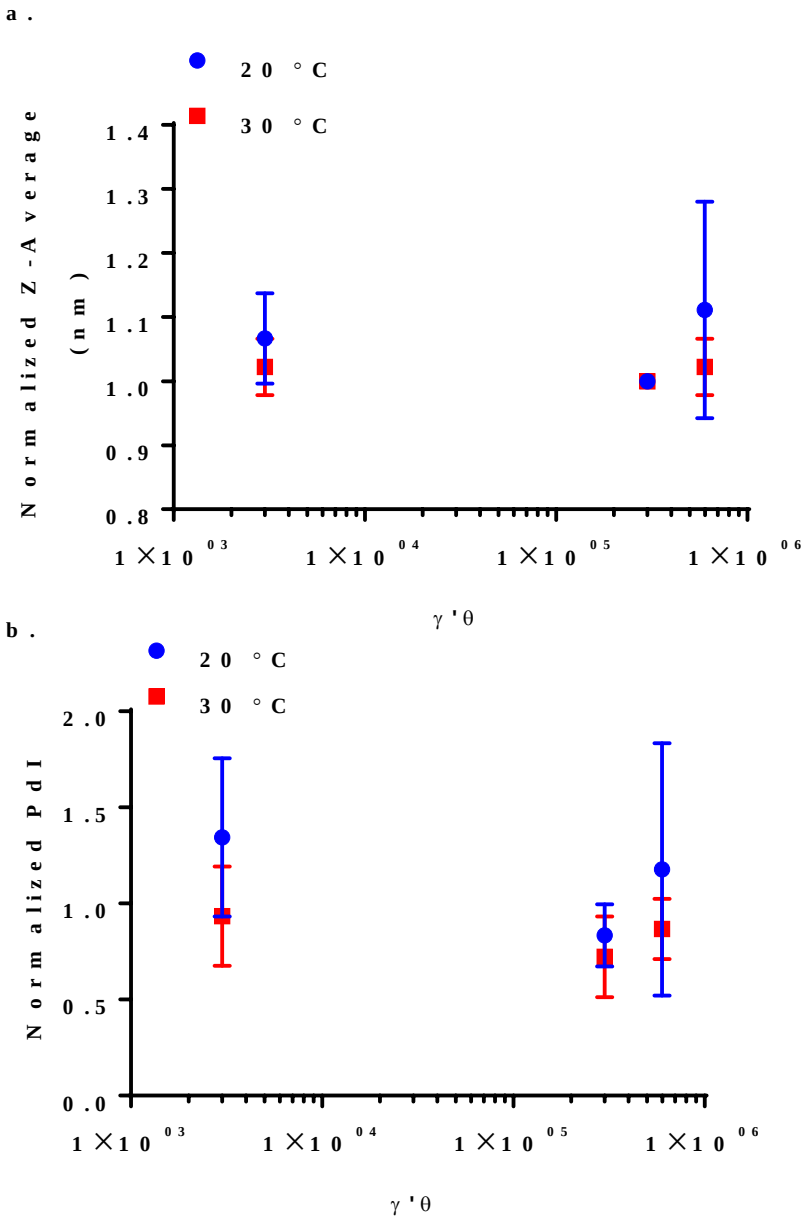

Figure 3. The effect of shear on the enzyme was measured using the rotational rheometer at both 20 °C and 30 °C. Normalized result to initial values from DLS testing: (a) hydrodynamic size as indicated by Z-Average values and (b) particle heterogeneity indicated by polydispersity index results.

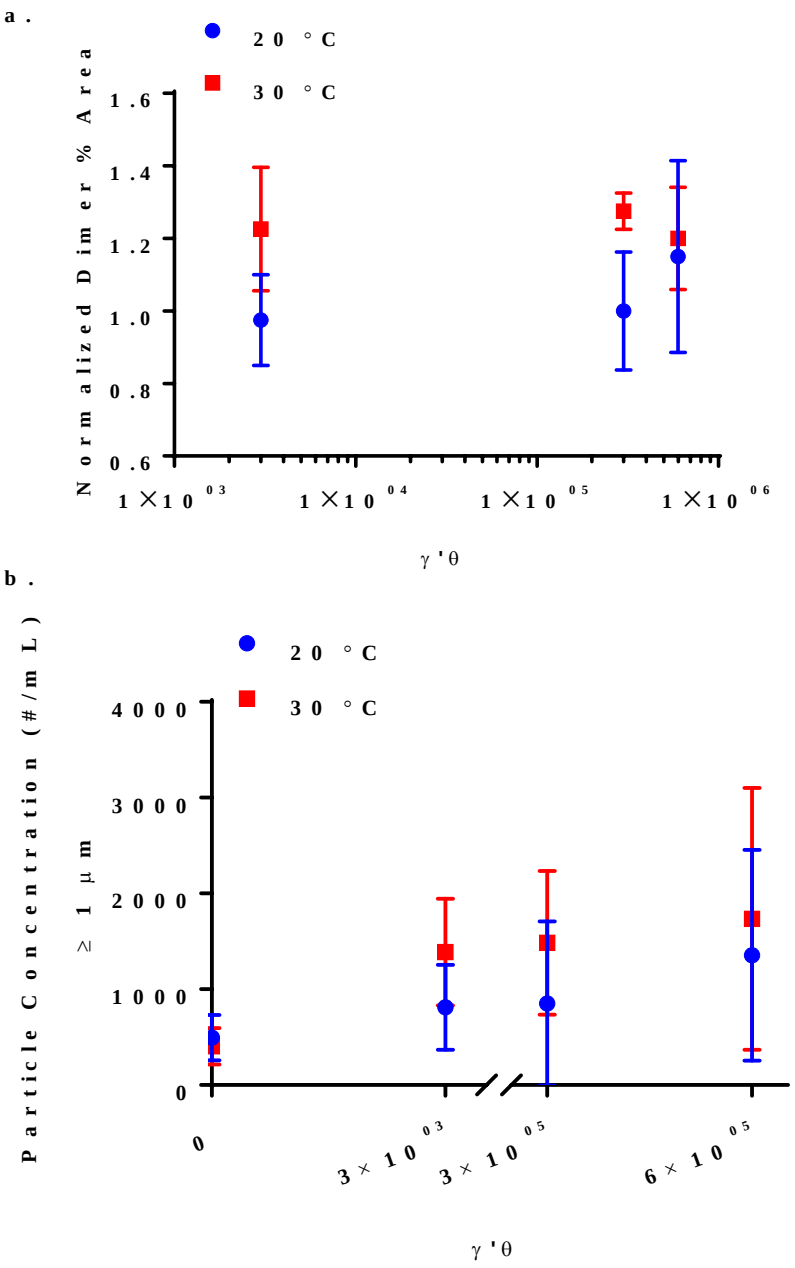

Figure 4. Results from rotational rheometer experiments at both 20 °C and 30 °C (a) SEC-HPLC % Area dimer. (b) MFI values for neat protein solution across all γ'θ values tested.

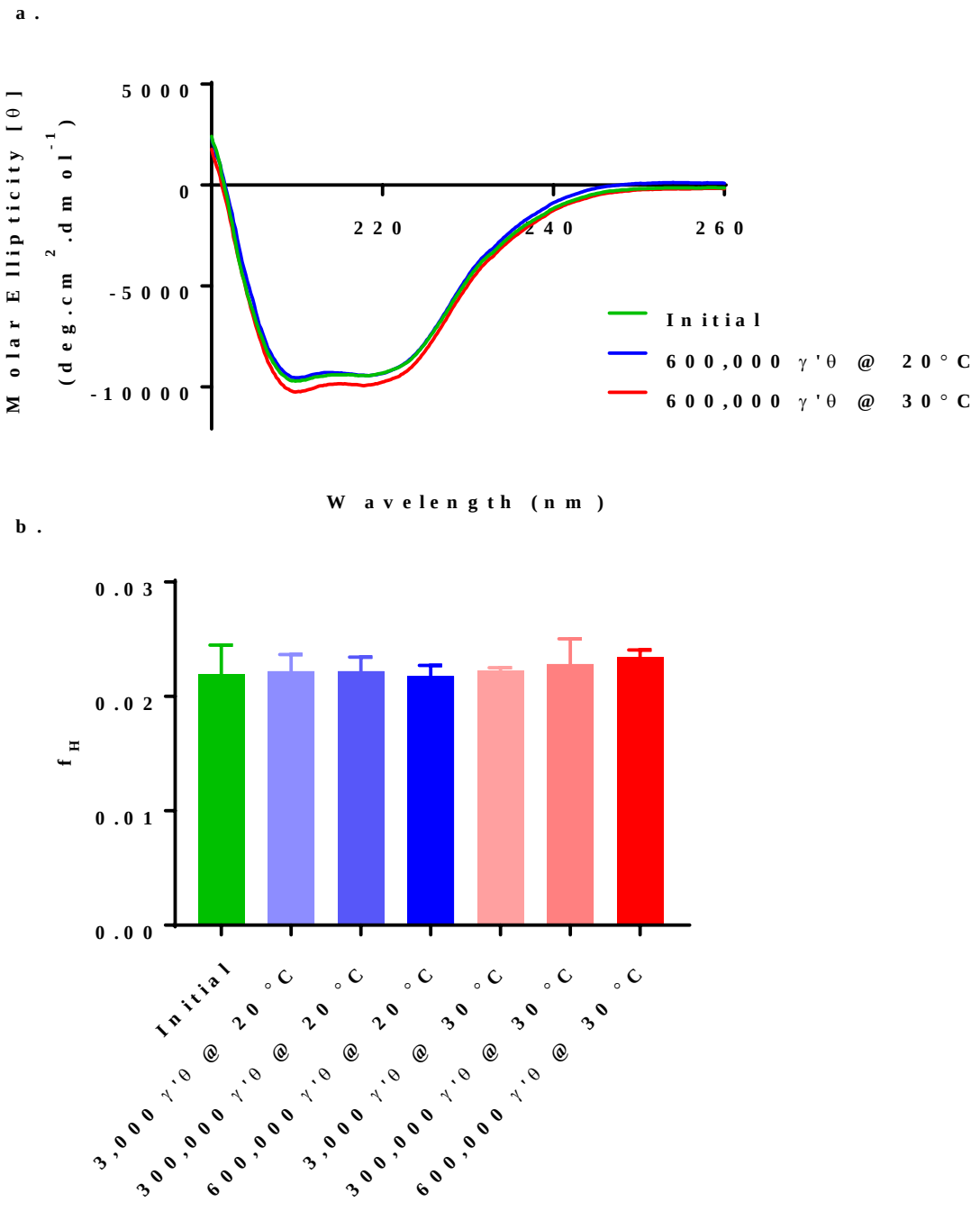

Figure 5. (a) Qualitative overlay of CD spectra, for highest stress scenarios by the rotation rheometer model. (b) Relative amounts of α-helical content, in terms of fraction helical (f_H).

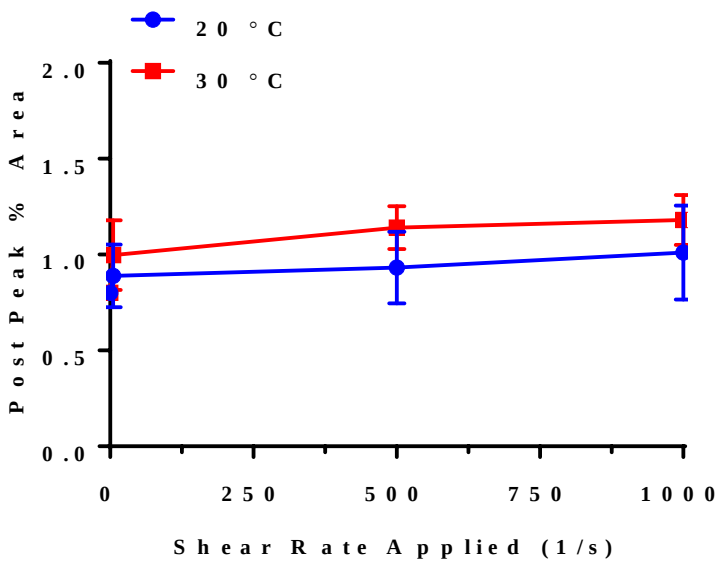

Figure 6. Effect of shear using the Rotational Rheometer as observed using reversed-phase HPLC. Post peak % area, shown *vs.* shear rate applied at both 20 and 30 °C.

C.3. Rotational Rheometer Results

The rotational rheometer experiments were carried out to model an applied shear stress with the addition of an air-solution interface. The results produced low responses measured overall, as seen in Figures 3–6. A small response was observed initially at 20 °C test conditions, so additional experimental replicates (n = 3) were performed to probe whether the responses were significant and reproducible. The rotational rheometer studies were also repeated at 30 °C, in attempts to exaggerate any instability introduced by this model. The results showed that an increase of 10 °C in temperature did not produce a significant instability across γ'θ parameters tested.

DLS analytical results can be seen in Figure 3a–b for both temperatures tested across γ'θ tested. When the Z average values were normalized to initial and averaged over 3 separate experiments, the result did not show a trend of signal increase with an increase in γ'θ parameters or with an increase in temperature. Normalized PdI shown in Figure 3b also displayed no change from initial, indicating that the rotational rheometer model did not cause significant non-native destabilization or aggregation as measured by light scattering.

SEC HPLC normalized dimer % area *vs.* increasing γ'θ are plotted in Figure 4a. The 20 and 30 °C linear regression analyses did not produce a slope significantly differ from zero, with *p*-values of 0.2472 and 0.7859, respectively. The linear regression analyses also revealed that the data for 20 and 30 °C were not significanly different from each other, with a *p*-value of 0.1874. SEC HPLC did not detect soluble enzyme aggregation or destabilization resulting from the rotational rheometer model experiments at either temperature.

Figure 4b displays the MFI SVP concentration *vs.* increasing γ'θ parameter and it illustrates a slightly positive correlation with γ'θ parameter; however, after statistical analysis the positively trending slopes were not significantly different from zero (*p*-values ≥ 0.0904). Additionally, the 20 and 30 °C lines were determined to not be significantly different from each other, with a *p*-value of 0.7764. Thus, it indicates that any observed fluctuations in SVP count by MFI can be explained due to random variance in the method. SEC, DLS and MFI have been established as orthoganol techniques to characterize aggregate particles of varying sizes. The results from these methods did not produce appreciable changes with increasing γ'θ, indicating that the rotational rheometer experiments, with the addition of an air-interface and reaching higher γ'θ parameters than the m-VROC™ model, did not induce measureable colloidal instability for this enzyme formulation.

CD was performed to evaluate whether there were global secondary structural changes in the enzyme during stressed conditions across γ'θ parameters at either experimental temperature (Figure 5a–b). As seen previously in the m-VROC™ results section (Figure 2a.), the enzyme contains α-helical secondary structure as indicated by the double minima at 208 and 222 nm (Figure 5a). Qualitatively, a comparison of the full spectral overlay for the initial and highest γ'θ at both 20 and 30 °C do not indicate visible difference from the initial spectra. For a quantitative comparison of the CD spectra upon increased γ'θ, the α-helical content (f_H) was calculated using the following calulation[17]:

$$[\theta]_{222} = -30{,}300\, f_H - 2340$$

where $[\theta]_{222}$ is the mean residue ellipticity at 222 nm. Figure 5b shows f_H for each of the stressed biotherapeutic conditions and compared to initial in green. No significant changes in the helical

structure from initial, as indicated by a series of one-way ANOVA tests, all resulted in *p*-values of 0.6242 or higher. CD was not able to resolve destabilization in secondary structure occurring from application of a shear stress using a rotational rheometer for this enzyme solution.

To evaluate the presence of chemical modifications to the enzyme, the RP-HPLC method was used to monitor % area of the post peak (Figure 6a–b). Figure 6a displays the raw post peak area % *vs.* shear rate applied for both 20 and 30 °C. Linear regression analysis of the 20 and 30 °C post peak % area data show that either slope are not significantly non-zero with a *p*-values of 0.0858, and 0.1625, respectively. Additionally, the 20 and 30 °C values are not significantly different from each other, *p*-value of 0.4227. The RP-HPLC results corroborate all the other analytical results to show that the rotational rheometer, at two different temperatures tested with reaching a maximum $\gamma'\theta$ of 6×10^5, did not induce measureable instability in the enzyme solution even with the addition of an air-interface

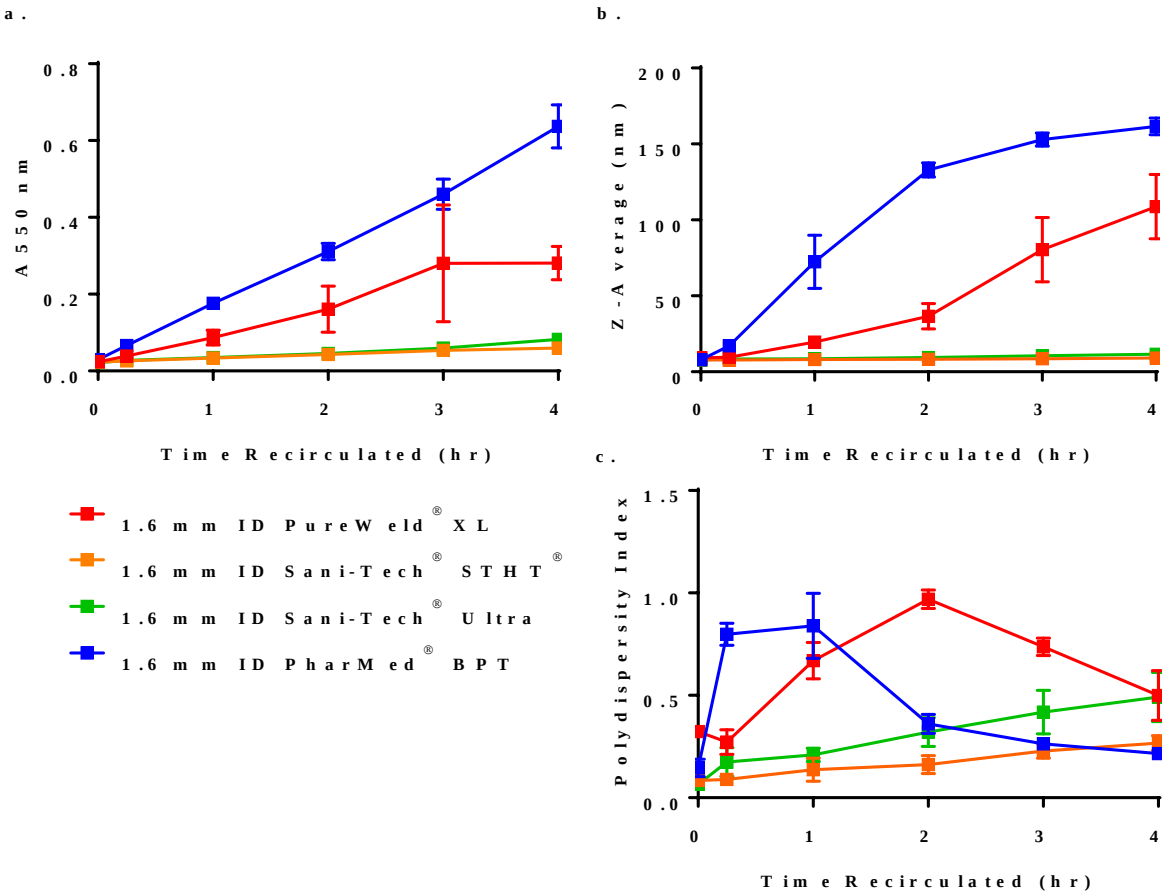

Figure 7. Bulk properties of the enzyme solution during recirculated pumping between 0 and 4 h through 1.6 mm ID tubings from PureWeld®XL, Sani-Tech®STHT, Sani-Tech®Ultra, and PharMed®BPT (n = 4). (a) Turbidity, (b) Z average, and (c) polydispersity index measurements after recirculating neat protein solution and diluted with 30 x aCSF buffer. Non-soluble aggregates removed using a 0.22 µm PVDF filter prior to analysis by DLS.

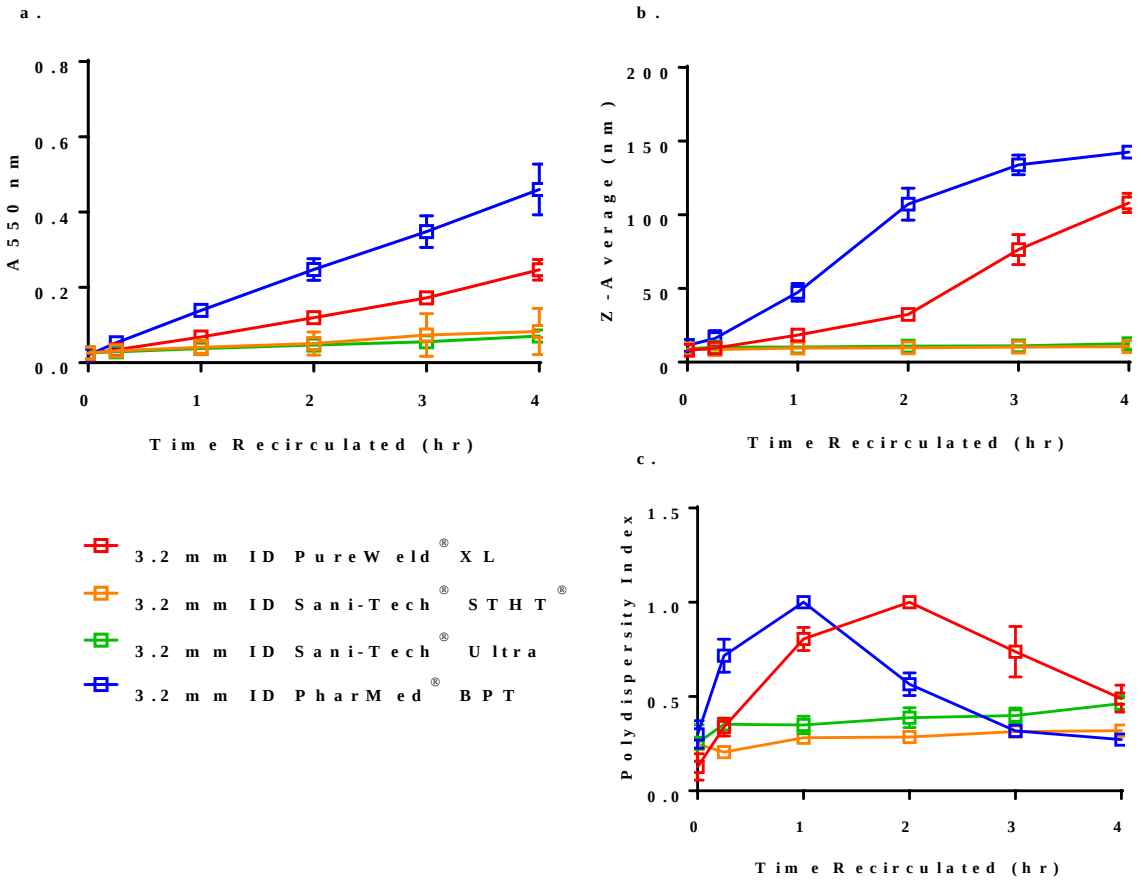

Figure 8. Bulk properties of the enzyme solution during recirculated pumping between 0 and 4 h through 3.2 mm ID tubings from PureWeld®XL, Sani-Tech®STHT, Sani-Tech®Ultra, and PharMed®BPT (n = 4). (a) Turbidity, (b) Z average, and (c) polydispersity index measurements after recirculating neat protein solution and diluted with 30 x aCSF buffer. Non-soluble aggregates removed using a 0.22 µm PVDF filter prior to analysis by DLS.

C.4. Recirculated Pumping Model Results

The pumping model simulates the transport of the enzyme solution via four different tubings: PureWeld®XL, Sani-Tech®STHT, Sani-Tech®Ultra, and PharMed®BPT at two inner diameters (*i.e.*, ID = 1.6 and 3.2 mm). These models reached the highest $\gamma'\theta$ parameter range (Table 3) and added interfacial complexity by using various tubing surfaces described in Table 4. The most obvious effect of pumping was the visually observed insoluble flocculated protein aggregates in the solution. Thus, turbidity of the solution was measured at 550 nm absorbance to quantify the property of the bulk solution throughout the experiment upon observation of visual aggregates (Figures 7a and 8a). The results all showed a significant, non-zero linear trend of increasing turbidity with time recirculated for all four tubing types at both sizes, with *p*-values ≤ 0.006. PharMed®BPT tubing performed the worst followed by PureWeld®XL tubing at both ID's tested. The silicone tubings, Sani-Tech®STHT and Sani-Tech®Ultra, perform much better than the thermoplastic elastomer tubings for identical experiments and are indistinguishable from each other.

Turbidity is a measurement of the bulk particulate properties of a system, similar to DLS measurements. However, for DLS measurements the enzyme solutions were diluted and filtered using a 0.22 μm PVDF filter to effectively limit the size scale of analysis and mitigate the intense light scattering caused by large insoluble aggregates. Interestingly, regardless of the tubing ID, the observed DLS results from each tubing trended incredibly closely to each other (Figures 7b and 8b). It appears that tubing chemistry dictates the Z-Average outcome over time pumped. Additionally, the DLS data corroborates with the turbidity results in tube ranking. PharMed®BPT and PureWeld®XL tubings caused the most dramatic increases in hydrodynamic

size, while the silicone tubings produced much slower and overall lower increases in hydrodynamic size.

The polydispersity index (PdI) in Figures 7c and 8c illustrate a similar trend with the Z-average results. After one hour of pumping, the PharMed®BPT sample reached essentially a PdI of one, indicating the presence of many differently sized particles in solution. Interestingly, the PdI values of these samples fell back towards a monodisperse system over time pumped, suggesting that the aggregates either coalesced into a single large enzyme aggregate or that they became insoluble and could not be detected either due to their removal during the 0.2 µm filtration prior to testing, or their settling to the bottom of the measurement cell during measurement. The PureWeld®XL pumped samples follow a similar trend, but after two hours of pumping, indicating either that the enzyme solution appears slighty more stable when exposed to pumping in PureWeld®XL tubing than PharMed®BPT or that they could be progressing through different mechanisms of aggregation. The Sani-Tech® silicone tubing PdI data could only be distinguished from each other in the PdI result sets, with the Ultra producing a slightly more polydisperse system than the Sani-Tech®STHT at both tubing IDs.

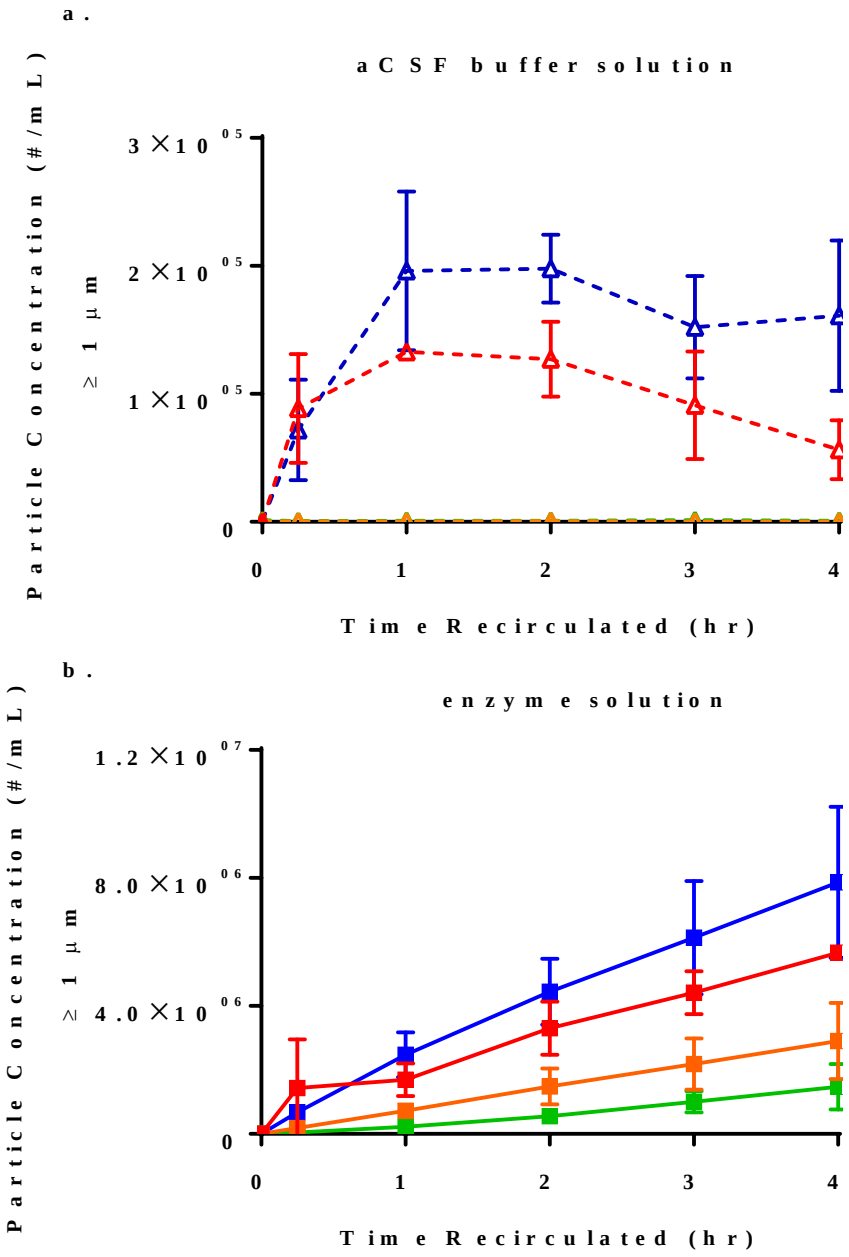

Figure 9. Total SVP concentrations measured after recirculation in 1.6 mm ID tubings in (a) aCSF buffer solution (n = 3) and (b) enzyme solution (n = 4). Tubing type are indicated by color including 1.6 mm ID Sani-Tech®Ultra (green), 1.6 mm ID PureWeld®XL (red), 1.6 mm ID Sani-Tech®STHT (orange) and 1.6 mm ID PharMed®BPT (blue).

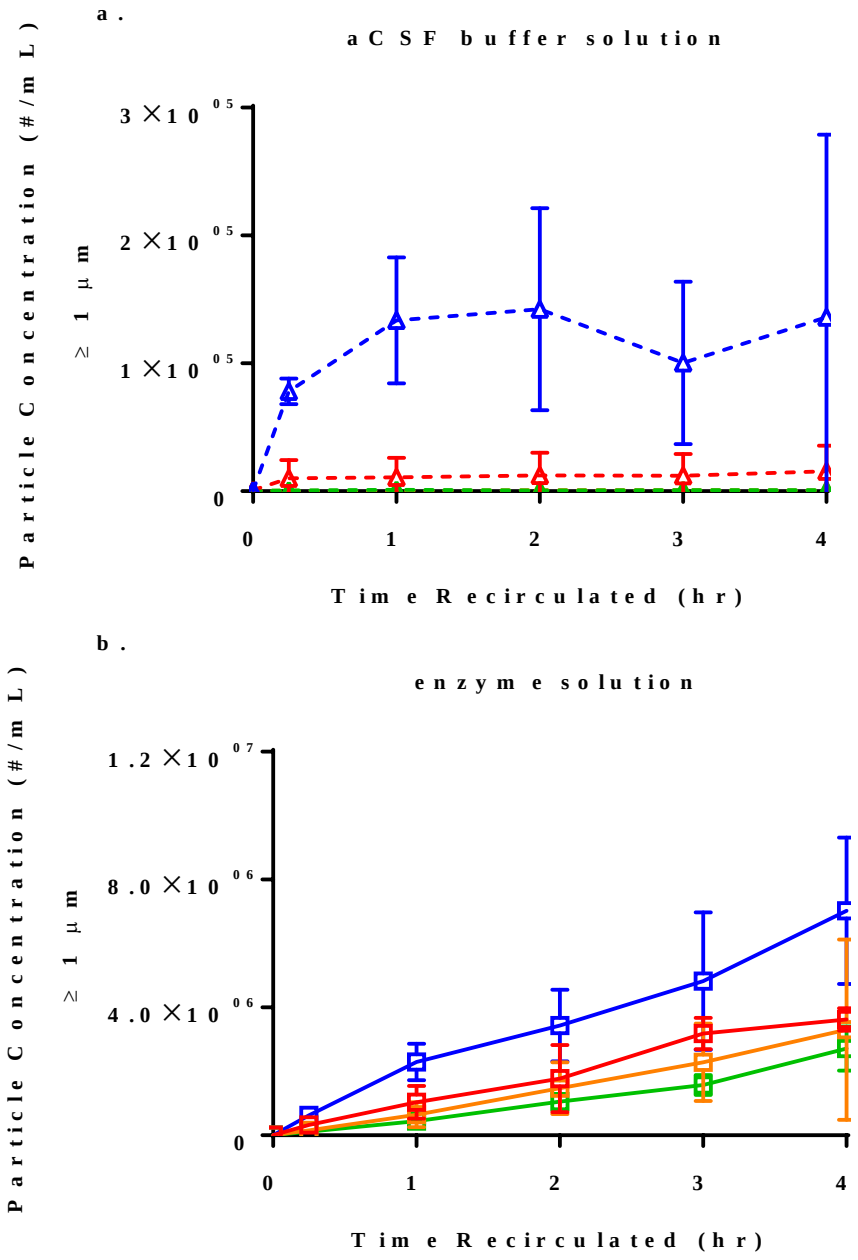

Figure 10. Total SVP concentrations measured after recirculation in 3.2 mm ID tubings in (a) aCSF solution (n = 3) and (b) biotherapeutic enzyme solution (n = 4). Tubing type are indicated by color including 3.2 mm ID Sani-Tech®Ultra (green), 3.2 mm ID PureWeld®XL (red), 3.2 mm ID Sani-Tech®STHT (orange) and 3.2 mm ID PharMed®BPT (blue).

Figures 9–10 show the mean and standard deviation observed for total SVP concentration from all recirculation study replicate experiments. aCSF buffer replicates (n = 3) were added to

these experiments to investigate only the effects of tubing degradation, and were indicated in Figure 9a and 10a. Both sizes of PharMed®BPT tubing consistently produced the highest SVP counts of all tubings tested for both aCSF and enzyme recirculated solutions. PureWeld®XL tubing produced a dramatic difference in SVP counts between the 1.6 mm ID tubing and the 3.2 mm ID tubing in the case of aCSF solution, indicating that the smaller 1.6 mm ID with the higher flow rate, leads to a higher incidence of tubing shedding than the 3.2 mm ID tubing. aCSF solution pumped through both PharMed®BPT and PureWeld®XL tubing reached an SVP concentration maximum threshold after approximately 1 hour. aCSF buffer solution pumped with silicone Sani-Tech® tubings produced remarkably low SVP's overall in comparison to the PharMed®BPT and PureWeld®XL using particles with 1–100 micron size range. This indicates a very low occurrence of tubing shedding in this particle size range.

MFI allows not only for the quantification of SVPs, but also captures images of each particle for qualitative morphological analysis. Theoretically, light proteinaceous particulate could be separated from darker tubing particulate caused by material shedding. However, from early on in these experiments, the resulting total particulate concentrations were too high and too diverse to reliably depend on morphological parameters to separate tubing SVPs from a mixture of tubing SVPs and enzyme aggregate SPVs. Therefore, the information gleaned from the data presented in Figures 9a. and 10a. serves as a control to understand the quality of the tubing itself. Clearly, the silicone tubings outperform the PharMed®BPT and PureWeld®XL tubing in the experiments with 1.6 ID tubings. In contrast, the experiments with a 3.2 mm ID tubing, PharMed®BPT tubing distinguishes itself as the worst performer in terms of SVP release in the presence of aCSF solution alone.

The pumped enzyme solutions, as seen in Figures 9b. and 10b., contain both shed tubing particles and SVPs resulting from insoluble protein aggregation. Overall, the solution pumped through 1.6 mm ID (Figure 9b) tubings trended slightly higher in SVP counts than the 3.2 mm ID tubings (Figure 10b), even with the different experimental volumes are taken into account. Similar to the aCSF solution results, the PharMed®BPT trended as the highest generator of SVP counts at both tubing sizes. The second highest SVP counts were again attributed to the PureWeld®XL tubing. Additionally, none of the recirculated enzyme solutions appeared to reach a threshold in SVP concentration as observed in the aCSF buffer experiments; however, a continued growth of SVP concentration was observed over time. Interestingly, although the 3.2 mm ID PureWeld®XL tubing for the aCSF buffer (red, Figure 10a.) showed a low level of SVP, the recirculated enzyme solution still resulted in high SVP counts.

The recirculated enzyme solution experimental results for SVP show only slight differences between the two silicone tubings. In the highest-stressed condition produced by the 1.6 mm ID tubing (Figure 9b.), Sani-Tech®Ultra tubing (green) trends to have slightly lower in SVP's than Sani-Tech®STHT tubing (orange). This trend was also observed for the 3.2 mm ID tubing recirculation replicates (Figure 10b.), indicating that the enzyme interaction with the tubing material could be slightly higher in Sani-Tech®Ultra than in Sani-Tech®STHT.

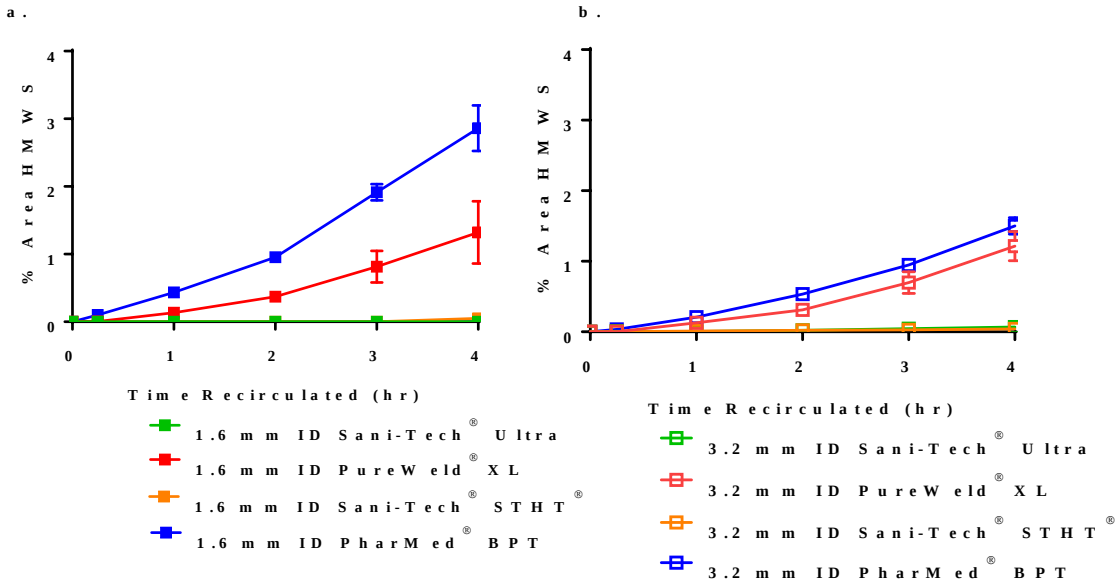

Figure 11. SEC high molecular weight species (HMWS) from enzyme solution recirculation experiments (a) 1.6 mm inner diameter (ID) tubing, and (b) 3.2 mm ID tubing of the same tubing types. All data reflect % area values from integrated chromatograms at 214 nm.

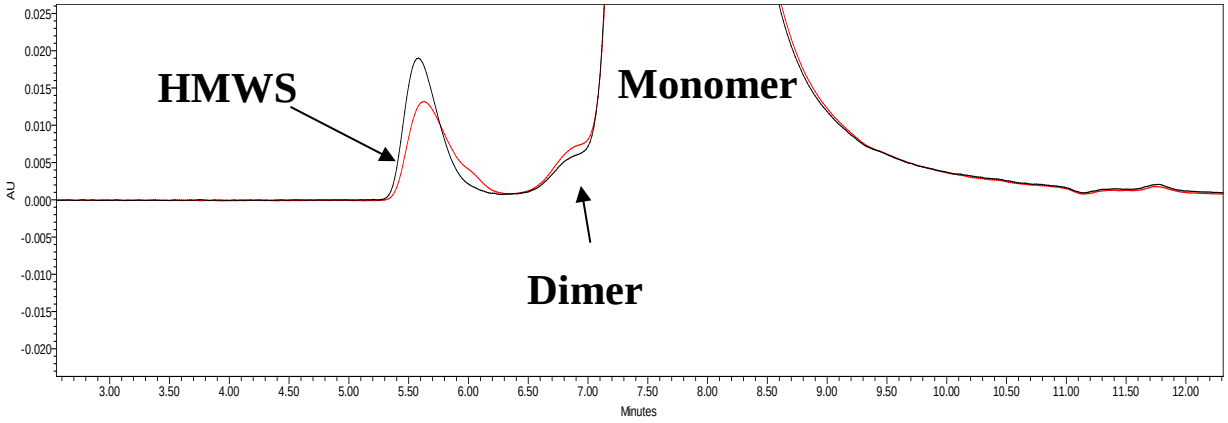

Figure 12. Recirculated enzyme solution representative of the worst-case in SEC chromatogram overlay of HMWS, dimer, and monomer from 4-hour pumped thermoplastic elastomer tubing

material experiments. The black trace represents PharMed®BPT tubing, and the red trace represents PureWeld®XL tubing material.

The SEC-HPLC method was employed to quantify the amount of soluble higher-order aggregates (% HMWS), dimer, monomer, and fragments in solution caused by pumping through various tubing experiments. The results provided a more resolved investigation of heterogeneity of the system than DLS, and is quantified by % Area at 214 nm. Figures 11a–b displayed the results from both tubing sizes and there was no trend observed in the Sani-Tech® tubings. In contrast, sharp increases were observed in the PureWeld®XL and PharMed®BPT tubings. In fact, PharMed®BPT tubing caused the most dramatic increase in HMWS content with detected levels of HMWS found after only 15-minutes of recirculated pumping. HMWS % area in PureWeld®XL also showed growth over time during recirculation process, but the HMWS became detectable after 1 hour. Overall, the smaller tubing ID experiments (Figure 11a) produced higher levels of HMWS than the larger tubing ID (Figure 11b), which could be attributed to, at least in part, the higher shear experienced at the tubing wall in 1.6 mm ID tubing.

Figure 12 displays an overlay of SEC chromatograms for the effects of the 4-hour recirculation on the enzyme solution using PharMed®BPT (black) and PureWeld®XL (red) tubings. The HMWS is the first peak to elute followed by a poorly resolved dimer at the shoulder of the monomer peak. The results from Sani-Tech® tubings were not included in Figure 12 because they did not produce a significant level of HMWS. There was no observable enzyme fragment in the recirculated samples. Additionally, the dimer peak % area remained constant through all the experiments completed in this work. Therefore, the most interesting find was the growth of the HMWS peaks in PharMed®BPT and PureWeld®XL tubings because the HMWS changed by growing in % Area with pumping time.

It is also interesting to note that the HMWS consistently generated by pumping with either the PharMed®BPT or PureWeld®XL appear to be slightly different species, as indicated by the

peak shape. The PharMed®BPT pumped samples produced a more gaussian peak, indicating a single species, while the PureWeld®XL HMWS peak always appeared bimodal. The HMWS produced in the PureWeld®XL tubing forms a more polydisperse range of higher order aggregates, indicating possible different aggregation pathways depending on the tubing chemistry.

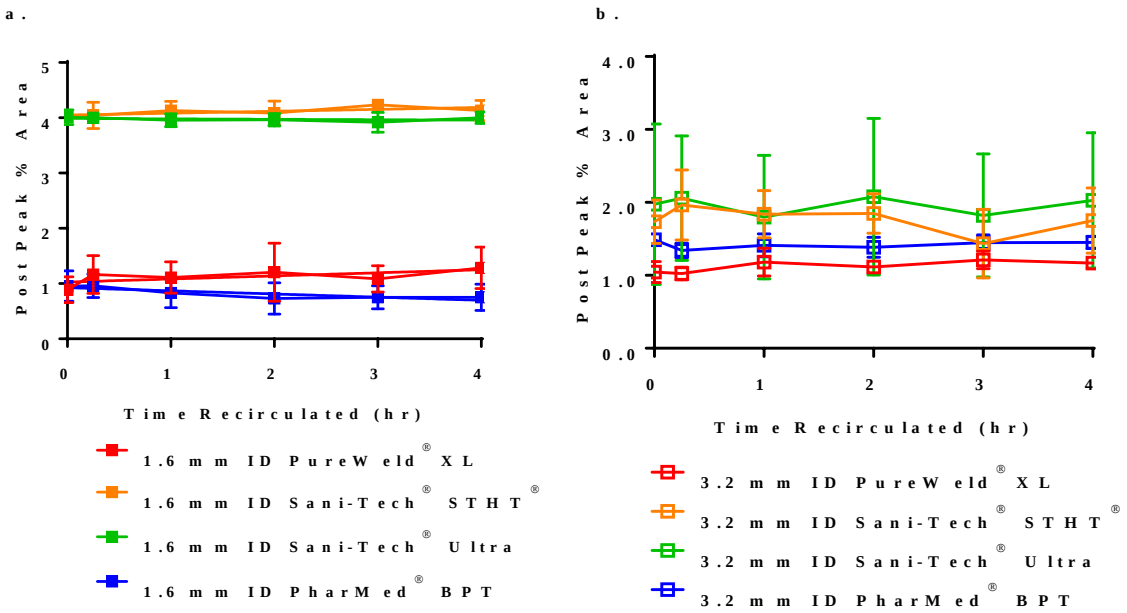

Figure 13. Quantified post peak % area from recirculation experiments (a) 1.6 mm inner diameter (ID) tubing and (b) 3.2 mm ID tubing of the same tubing types. All data reflect integrated chromatograms at 214 nm.

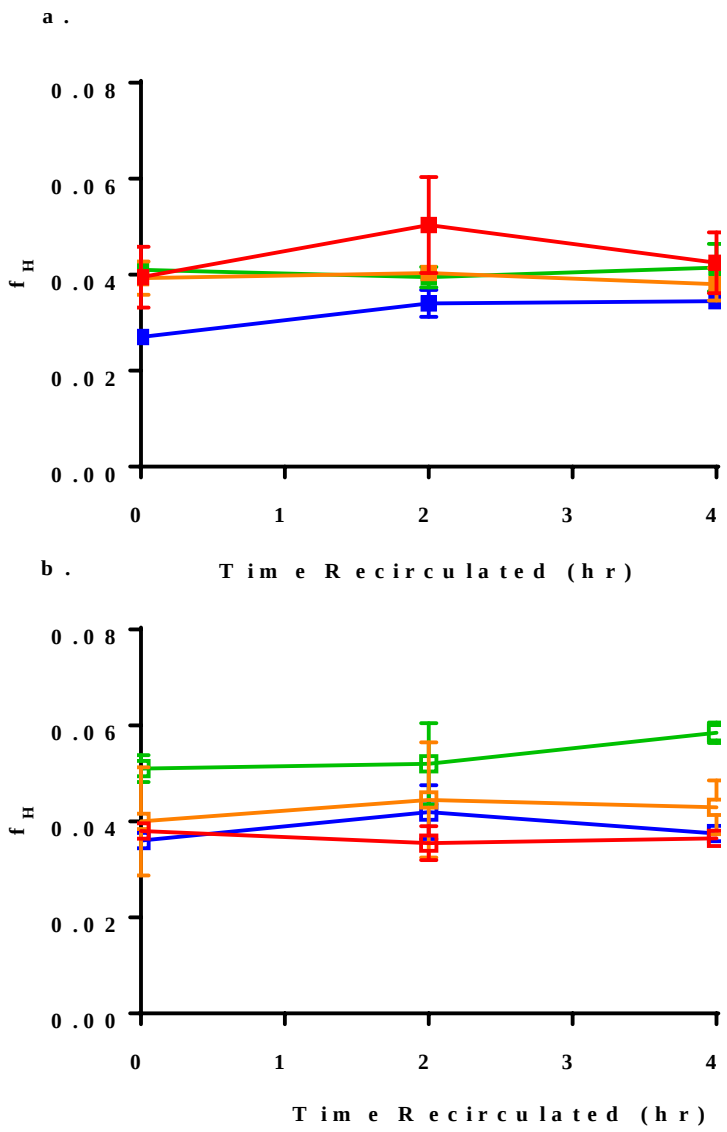

Figure 14. α-helical content (f_H) from recirculation experiments (a) 1.6 mm ID tubing (filled squares) and (b) 3.2 mm ID tubing (open squares) of each tubing type. Tubing type are indicated by color including Sani-Tech®Ultra (green), PureWeld®XL (red), Sani-Tech®STHT (orange) and PharMed®BPT (blue). CD experiments completed for two independent experiments and only the 2-hour and 4-hour time points were tested.

The RP-HPLC method was employed to screen for possible chemical degradation caused by a combination of shear forces involved with pumping and exposure to various tubing surface chemistries. Specifically, an increase in post peak has been described to indicate changes in protein chemical stability (data not shown). The post peak was monitored throughout all the experiments and the data can be seen in Figure 13a and b for both tubing sizes tested. No significant growth in post peak was observed during pumping time; the linear regression analysis for every curve's slope showed no significant change from zero with *p*-values all ≥ 0.0270. The chemical modifications during shear and interfacial stresses were evaluated using RP-HPLC and there was no significant effect found across all models. Thus, the remainder of this work was focused on physical stability of the biotherapeutic enzyme.

CD experiments were used to assess the structural comparability of the recirculated enzyme solution across the various tubings. As the solutions were not filtered prior to far-UV CD measurements, the goal was to gain insight into the global secondary structure content in solution, which would also include higher order aggregates. In Figure 14a and b, the initial α-helical content (f_H) is plotted with 2-hour and the worst-case 4-hour recirculated solution. For all experiments, the resultant changes are insignificant from zero time point to 4-h time point with *p*-values of ≥ 0.2550, indicating there was no measurable change in secondary structure in this method.

D. DISCUSSION

The results exhibit the importance of examining physical stability of an enzyme during fill-finish processing in the absence of stabilizing excipients. Several different models were used to separate the effect of shear and interfacial interactions. Hydrodynamic flow effects alone did not appear to damage the enzyme in the m-VROC™ model, and neither did the addition of an air interface in the rotational rheometer model of shear stress. The recirculation pumping model, however, produced dramatic measurable changes in the enzyme's physical stability. Results indicate that physical stability of the enzyme solution were affected most significantly by enzyme-tubing surface interactions with less contribution from hydrodynamic forces on the enzyme structure.

In the recirculated pumping experiments, it is clear that Platinum-cured silicone surfaces (Sani-Tech®Ultra & Sani-Tech®STHT) produced drastically lower degradation effects than that of the thermoplastic elastomer (PharMed®BPT and PureWeld®XL) tubings. In manufacturing, PharMed®BPT tubing is frequently used in conjunction with peristaltic pumps due to its preferred durability, chemical resistance, and biocompatibility. However, the highest levels of SVP's were found in PharMed®BPT tubing pumped with aCSF buffer solution alone (Figures 9a & 10a), indicating that particles were shed directly from the tubing. PharMed®BPT tubing is a polypropylene based matter manufactured with mineral oil and other unknown blend materials that are hydrophobic in nature. The overall property of the tubing surface is hydrophobic; thus, it is necessary to coat it with hydrophilic poly-vinyl alcohols (PVA)[18]. The generation of particulate during recirculation of the aCSF buffer could be due to the disintegration of the hydrophilic coating, compromising the tubing by exposing its hydrophobic surface, and possibly promoting undesireable hydrophobic interations in the enzyme solution. Not only would the

tubing interface be hydrophobic, but the shed particles would be, as well. The released hydrophobic particles could act as aggregation nucleators, which is alarming because the use of this tubing is prolific in filling of many biotherapeutic products.

The PureWeld®XL tubing with 1.6 mm ID consistently produced a high SVP concentration in recirculated aCSF buffer solution at the highest volumetric flow rates (Figure 9a). In contrast, no overwhelming increase was observed in SVP's at 3.2 mm ID PureWeld®XL tubing (Figure 10a). A possible explanation for the difference in SVP amounts could be due to the difference in volumetric flow rates between the two tubing sizes. The rate differences led to a difference in pressure drop (ΔP) from 4.2×10^6 mPa for 1.6 mm ID to 0.9×10^6 mPa for 3.2 mm ID tubings. The higher pressure in a smaller tubing generates higher friction between the solution and the tubing surface, leading to the sloughing-off of particles from the tubing surface into solution. However, a difference of pressure drops may not be the only factor affecting the particle shedding from the surface. Another explanation originates from the physical appearance of the tubing surface itself. A rougher surface may cause important differences in the flow or friction interactions between the pumped liquid and the tubing wall, and may cause higher particle shedding. In a similar experiment done by Saller, *et al*., it was noted that surface roughness was a determining factor for particle shedding from silicone tubing as measured by 3D laser scanning microscopy, and that higher roughness of the suface led to higher production of particles.[19] If for any reason the internal tubing surface varied between the two ID sizes, differences in surface roughness could offer an explanation for the difference in shedding behavior, with the pressure drop differences only confounding the end result. Additionally, continuous peristaltic recirculation pumping for up to 4-hours visually deformed the external surface of every type of tubing in these studies, indicating the friction between the the tubing with the peristaltic pump

rollers could be a large source of SVP measured. Internal spallation could also occur due to squeezing action by the rollers; with the smaller tubing exhibiting more spallation, as there would be less surface area in the pumphead, and therefore higher forces involved pressing onto the tubing material. An important consideration from these data is the fact that the two tubing sizes exhibited different behaviors. This indicates that individual testing with this particular material should be always be performed and the use of PureWeld®XL as a candidate for fill-finish should be approached with caution.

Additional limitations should be considered as well for the PureWeld®XL, especially in terms of behavior of the tubing in the pumphead. In these studies, the PureWeld®XL tubing was difficult to keep in the pumphead during pumping process due to its smooth surface; the tubing continuously traveled through the pumphead, causing stops in the experiment for tubing repositioning. Another reason that PureWeld®XL should perhaps be disregarded in consideration as a candidate for a manufacturing operation involving peristaltic pumping.

The large increases in SVP caused in enzyme solution by tubing materials can be explained by two main pathways. First, a hydrophobic thermoplastic elastomer surface alone can pose a risk for inducing aggregation. A native enzyme could experience a reversible and non-specific binding event to the surface via interaction with the hydrophobic core of the enzyme, which can induce partial unfolding in solution.[20] Once the conformationally compromised enzyme is released back into solution, it is susceptible to subsequent oligomerization processes. Additionally, because shed SVP's the from surface coating disintegration could be hydrophobic in nature, these particles can act as heterogeneous nucleation sites for enzyme aggregation away from the tubing surface. Although the sub-visible range shed particulates could be filtered from the product, the generated soluble aggregates (*i.e.*, HMWS) could pass through a sterile filter,

and would be included in the final drug product. The presence of soluble HMWS in the final product increases the risk for subsequent aggregation events during shelf-life including shipping/handling prior to administration of the product. Thus, there is need for close monitoring of the product to ensure a safe and efficacious drug on stability.

A similar trend was observed for concentration of SVP's in the enzyme solution after recirculation with thermoplastic elastomer tubings; in this case, SVP concentrations were much higher than platinum-cured silicone tubings (Figures 9b & 10b). On one hand, it is easy to understand this phenomenon as the thermoplastic elastomer material with buffer alone produced SVP's; therefore, the SVP's are also expected to be present in the recirculated enzyme solution. However, the enhanced particulate growth in the enzyme solution was far past what was seen in aCSF buffer recirculated solution. This enhancement could be a combination of several factors with the largest factors being protein interactions or collisions with tubing surface or shed floating particulates. At the 4-hour time point for both tubing sizes, the concentration of aggregates were higher in PharMed®BPT and PureWeld®XL compared to the other two tubings (Sani-Tech®Ultra & Sani-Tech®STHT) as reflected globally by turbidity (Figures 7a & 8a) and Z-average (Figure 7b & 8b) measurements. The levels of aggregation at the 4-hour time point for both Sani-Tech®Ultra & Sani-Tech®STHT remained low in all recirculation experiments. A similar trend has also been reported by Mahajan *et al*. between Platinum-cured silicone tubing and polypropylene based tubing with USP mineral oil in recirculation experiments performed with virus-like particles adsorbed to adjuvant[21]. The data from Mahajan *et al*. showed that pressure at 0–3.5 psi was not a factor in causing increased particle size change (%) but the observed dramatic increase in particles was caused by tubing material[9]. This study showed that

the silicone tubing outperformed the polypropylene material by producing much lower increases in particle size regardless of pressure.

These observed optical data were also supported by SEC (Figure 11), showing that both PharMed®BPT and PureWeld®XL produced multimer peaks which were not detected in the silicone tubings. The HMWS present from PharMed®BPT and PureWeld®XL were even different from each other as shown in Figure 12. The difference in the multimer peaks could indicate that the mode of degradation experienced as a result of elastomer surface could depend on tubing type; thefore indicating that tubing chemistry influences the physical degradation observed. In an extractable/leachable study conducted by Jenke, *et al.* it was shown from simulated use experiments that silicone tubings produced a different leachable profile than Santoprene-type tubings, with the Santoprene introducing alkylphenols and decomposition products of Irganox-type antioxidants[22]. Athough the silicone tubings and Santoprene-type (thermoplastic elastomer) tubing identities and manufacturers were not disclosed, it is evident that the elastomer tubing leachables, as they are unique from silicone, could also be implicated as heterogeneous nucleating agents in solution, possibly leading to the observed soluble HMWS.

The polydispersity in the enzyme solution was also an indicator of unique aggregation kinetics produced by either the PharMed®BPT and PureWeld®XL tubings (Figures 7c & 8c). The enzyme solution in PharMed®BPT tubing reached a maximum PdI after only 15 minutes of recirculation compared to the 2 hours in the PureWeld®XL tubing. For both PharMed®BPT and PureWeld®XL tubings, the polydispersity dropped after reaching a maximum. This observation was presumably due to the precipitation of larger aggregates that were filtered out of the solution prior to analysis with the 0.22 µm filter.

One of the goals of this work was to not only point out the inherent risk involved with formulating an ERT in the absence of stabilizing excipients, but also to highlight that certain risks can be mitigated by implementing proper processes. One of the most simplistic mitigation strategies is to use the most appropriate tubing chemistry from the beginning during the process design. In addition, enzyme degradation data could be used to convince tubing manufacturers to release additional information about tubing surface chemistry to help elucidate problems of protein instability. This would allow pharmaceutical scientists to narrow the selection of tubings that are appropriate for a specific biotherapeutic protein without such exhaustive experimental studies; however, because the unique protein structure plays such a large role in protein surface interactions, individual tubing evaluation should still be completed. These experimental data should help drive decisions in the fill-finish process when working with entities within or outside an organization.

Often, tubing materials are selected based on in-house availability or preference for manufacturing convenience without a holistic consideration for compatibility with the biotherapeutic being delivered. Especially in the absence of stabilizing excipients, the results presented here underscore the need to investigate the possibility of inherent interfacial incompatibility that could exists between tubing surface and enzyme. One could imagine that a soluble aggregate below 0.22 µm would survive sterile filtration, and exist in the final drug product, threatening to be a destabilizing force for long-term stability. In a previous study by Saller *et al*.[19], it was reported that silicone tubing used in recirculation studies produced around 200 nm particles, which could pass through the sterile filtration process. Irrespective to the production of nano particulate, it was demonstrated that the silicone tubing particulate did not show an additive effect to the degradation of two separate mAb formulations[23]. However, it

should also be noted that these formulations included stabilizing agents such as sugar and nonionic surfactants to mitigrate deleterious surface interactions. A similar spiking study with long-term stability may be an important piece of information for an enzyme formulation with no stabilizing sugars and surfactants. Protein stability in terms of efficacy alone is only one piece of the equation, it is also imperative to demonstrate safety of the product, because aggregate species can be responsible for adverse immune responses[24]. It is a simple and easy solution to replace incompatible tubing with a compatible tubing to produce a safer and more stable drug product.

An interesting set of follow-up experiments to this work would be to add a sugar or surfactant to observe whether it would suppress the appearance of the multimer peak. A study conducted using a cone and plate rotational rheometer to apply a shear stress by Patapoff and Esue showed that the addition of polysorbate 20 reduced the formation of insoluble aggregates[25]. The study concluded that the decreased in aggregation was due to protection of protein form both air-water interface and shear stress[25]. Although aggregation was not observed in the rotational rheometer method in these experiments, it has also been shown that nonionic surfactants can prevent aggregation caused by many types of interfacial interactions other than the air-water interface interaction[1]. Therefore, it would be interesting to observe an increased in stability of our enzyme with added surfactants to further support the idea that the tubing material interface alone caused the observed aggregation effects in this study.

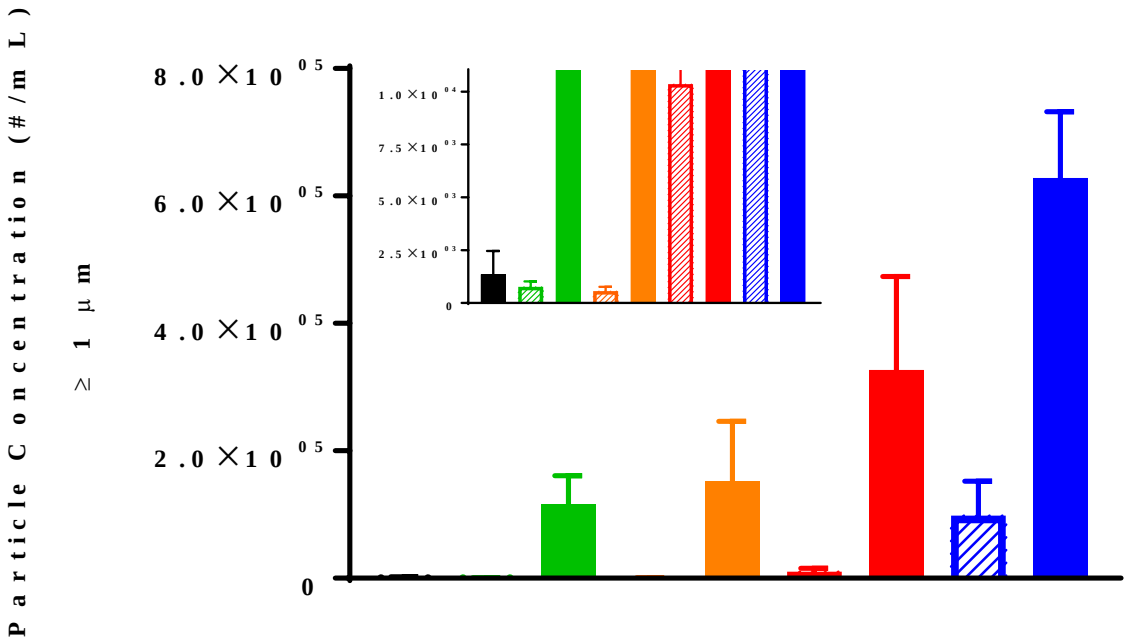

Figure 15. SVP concentration from MFI compared across models. Solid bars represent results from enzyme solution experiments, the rotational rheometer (black) had a $\gamma'\theta$ value of 6 x 10^5. Colored striped (aCSF buffer), and solid (enzyme solution) bars represent recirculation tubing experiments at 3.2 mm ID, with a $\gamma'\theta$ value of 5 x 10^5: Sani-Tech®Ultra (green), Sani-Tech®STHT (orange), PureWeld®XL (red), and PharMed®BPT (blue).

Clearly from the recirculation experiments, the Platinum-cured silicone tubings tested here are the superior for processes involving this enzyme solution without excipients. This finding could most likely be extended to other biopharma products. Theoretically, the rotational rheometer experiment at a $\gamma'\theta$ value of 6 x 10^5 could be most closely compared to the 3.2 mm ID tubing experiments at the 15-minute time point with a $\gamma'\theta$ value of 5 x 10^5 (Figure 15). In Figure

15, it is clear that the rotational rheometer results were not comparable in SVP concentration to that of recirculation experiments. The difference indicate that interfacial phenomena contributes greatly in the formation of SVP aggregates. It should also be noted that the use of the $\gamma'\theta$ parameter could be too simplistic to compare between the models because the recirculation model involves stresses generated by tubing, peristaltic pumping, and other forms of stresses including back pressure, micro-cavitation, or trapped air bubbles.

E. CONCLUSIONS

Three unique models were used to understand various stresses involved with the fill-finish process for an enzyme therapeutic. In this thesis, an m-VROC™ differential pressure viscometer, a rotational rheometer, and a peristaltically pumped recirculation model with common tubing materials were used to that end. The m-VROC™ and rotational rheometer experiments did not appear to introduce instability to the tested enzyme molecule system, indicating that the levels of hydrodynamic stress in these methods were below the levels required for denaturation, even with the addition of an air-interface in the rotational rheometer testing. However, the peristatic recirculation model produced clear trends in colloidal enzyme stability. A ranking exists among the types of tubings studied in the recirculation experiments. PharMed®BPT and PureWeld®XL produced the highest SVP counts in both buffer alone and the enzyme solution and are not the appropriate choice in manufacturing and fill-finish operations for the enzyme tested. These tubings have been shown to promote enzyme aggregation during a peristaltic pumping process, both soluble and insoluble aggregates were discovered. The Platinum-cured silicone tubing perfomed the best in these recirculation experiments and are optimal for manufacturing and fill-finish operations without major difference between the two types: Sani-Tech®STHT or Sani-Tech®Ultra.

F. REFERENCES

[1] CHI, E. Y. et al. Physical stability of proteins in aqueous solution: mechanism and driving forces in nonnative protein aggregation. **Pharmaceutical research,** v. 20, n. 9, p. 1325-1336, 2003 ISSN 0724-8741.

[2] CLELAND, J. L.; POWELL, M. F.; SHIRE, S. J. The development of stable protein formulations: a close look at protein aggregation, deamidation, and oxidation. **Critical reviews in therapeutic drug carrier systems,** v. 10, n. 4, p. 307-377, 1993. ISSN 0743-4863.

[3] NARHI, L. O. et al. Classification of protein aggregates. **Journal of pharmaceutical sciences,** v. 101, n. 2, p. 493-498, 2012 ISSN 0022-3549.

[4] PHILO, J. S.; ARAKAWA, T. Mechanisms of protein aggregation. **Current pharmaceutical biotechnology,** v. 10, n. 4, p. 348-351, 2009 ISSN 1873-4316.

[5] FROKJAER, S.; OTZEN, D. E. Protein drug stability: a formulation challenge. **Nature reviews. Drug discovery,** v. 4, n. 4, p. 298-306, 2005 ISSN 1474-1776.

[6] RATANJI, K. D. et al. Immunogenicity of therapeutic proteins: Influence of aggregation. **Journal of Immunotoxicology,** v. 11, n. 2, p. 99-109, 2014. ISSN 1547691X. Disponível em: < http://search.ebscohost.com/login.aspx?direct=true&db=a9h&AN=94970441&site=ehost-live >.

[7] SCHELLEKENS, H. Factors influencing the immunogenicity of therapeutic proteins. **Nephrology, dialysis, transplantation,** v. 20, n. suppl_6, p. vi3-vi9, 2005 ISSN 0931-0509.

[8] HERMELING, S. et al. Structure-immunogenicity relationships of therapeutic proteins. **Pharmaceutical research,** v. 21, n. 6, p. 897-903, 2004 ISSN 0724-8741.

[9] THOMAS, C. R.; GEER, D. Effects of shear on proteins in solution. **Biotechnology Letters,** v. 33, n. 3, p. 443-456, 2011/03/01 2011. ISSN 0141-5492. Disponível em: < http://dx.doi.org/10.1007/s10529-010-0469-4 >.

[10] BEE, J. S. et al. Aggregation of a monoclonal antibody induced by adsorption to stainless steel. **Biotechnology and bioengineering,** v. 105, n. 1, p. 121-129, 2010 ISSN 0006-3592.

[11] WILKES, J. O. **Fluid Mechanics for Chemical Engineers**. 2. Westford, Massachusetts: Prentice Hall Professional Technical Reference, 2009. ISBN 0-13-148212-2.

[12] BEE, J. S. et al. Effects of surfaces and leachables on the stability of biopharmaceuticals. **Journal of pharmaceutical sciences,** v. 100, n. 10, p. 4158-4170, 2011 ISSN 0022-3549.

[13] MAA, Y.-F.; HSU, C. C. Protein denaturation by combined effect of shear and air-liquid interface. **Biotechnology and Bioengineering,** v. 54, n. 6, p. 503-512, 1997. ISSN 1097-0290. Disponível em: < http://dx.doi.org/10.1002/(SICI)1097-0290(19970620)54:6<503::AID-BIT1>3.0.CO >.

[14] SLUZKY, V.; KLIBANOV, A. M.; LANGER, R. Mechanism of insulin aggregation and stabilization in agitated aqueous solutions. **Biotechnology and bioengineering,** v. 40, n. 8, p. 895-903, 1992 ISSN 0006-3592.

[15] CHARM, S. E.; LAI, C. J. Comparison of ultrafiltration systems for concentration of biologicals. **Biotechnology and bioengineering,** v. 13, n. 2, p. 185-202, 1971 ISSN 0006-3592.

[16] MCCABE, W. L.; SMITH, J. C.; HARRIOTT, P. **Unit Operations of Chemical Engineering**. New York: McGraw-Hill, 1993.

[17] CHEN, Y. H.; YANG, J. T.; MARTINEZ, H. M. Determination of the secondary structures of proteins by circular dichroism and optical rotatory dispersion. **Biochemistry (Easton),** v. 11, n. 22, p. 4120-4131, 1972 ISSN 0006-2960.

[18] XU, H.; SHULER, M. L. Quantification of chemical-polymer surface interactions in microfluidic cell culture devices. **Biotechnology progress,** v. 25, n. 2, p. 543-551, 2009 ISSN 8756-7938.

[19] SALLER, V. et al. Particle Shedding from Peristaltic Pump Tubing in Biopharmaceutical Drug Product Manufacturing. **Journal of Pharmaceutical Sciences,** v. 104, n. 4, p. 1440-1450, 2015. ISSN 1520-6017. Disponível em: < http://dx.doi.org/10.1002/jps.24357 >.

[20] KIESE, S. et al. Shaken, not stirred: mechanical stress testing of an IgG1 antibody. **Journal of pharmaceutical sciences,** v. 97, n. 10, p. 4347-4366, 2008 ISSN 0022-3549.

[21] MAHAJAN, R. et al. **Process Development Approach To Assess The Effect Of Formulation And Filling Processes On Physical Stability Of Biological Liquid Formulations**. The 2007 Annual Meeting: Merck, Sharp and Dohme Corp 2007.

[22] JENKE, D. R.; STORY, J.; LALANI, R. Extractables/leachables from plastic tubing used in product manufacturing. **International journal of pharmaceutics,** v. 315, n. 1-2, p. 75-92, 2006 ISSN 0378-5173.

[23] SALLER, V. et al. Influence of particle shedding from silicone tubing on antibody stability. **Journal of pharmacy and pharmacology,** v. 70, n. 5, p. 675-685, 2018 ISSN 0022-3573.

[24] ROSENBERG, A. S. Effects of protein aggregates: an immunologic perspective. **The AAPS journal,** v. 8, n. 3, p. E501-E507, 2006 ISSN 1550-7416.

[25] PATAPOFF, T. W.; ESUE, O. Polysorbate 20 prevents the precipitation of a monoclonal antibody during shear. **Pharmaceutical development and technology,** v. 14, n. 6, p. 659-664, 2009. ISSN 1083-7450.